GeV-TeV charged CR propagation models

Observational results & new trends

Pierre Salati – Université de Savoie & **LAPTH**

Outline

1) Introduction – cosmic rays & dark matter

2) The importance of multi–messenger analyses

3) Magnetic turbulence & CR diffusion – a bubbling field

4) Stochastic CR fluxes and the Myriad model

1) Introduction – cosmic rays & dark matter

Weakly Interacting Massive particles – WIMPs – may be the major component of the haloes of galaxies. Their mutual annihilations would produce an indirect signature of high–energy cosmic rays :

$$\chi + \chi \longrightarrow q\bar{q}, W^+W^-, \ldots \longrightarrow \gamma, \bar{p}, \bar{D}, e^+ \ \& \ \nu's$$

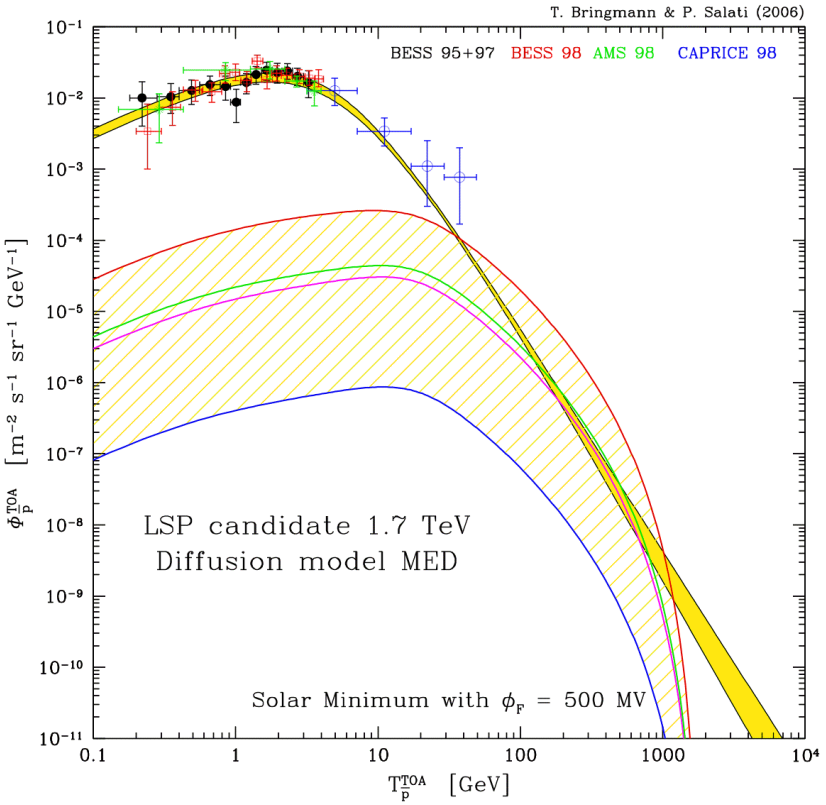

$M \longrightarrow \bar{p}, \bar{D}, e^+ + X$

Antimatter is already manufactured inside the galactic disk

Milky–Way seen by a cosmic–ray physicist

Cosmic rays propagate inside a diffusive halo

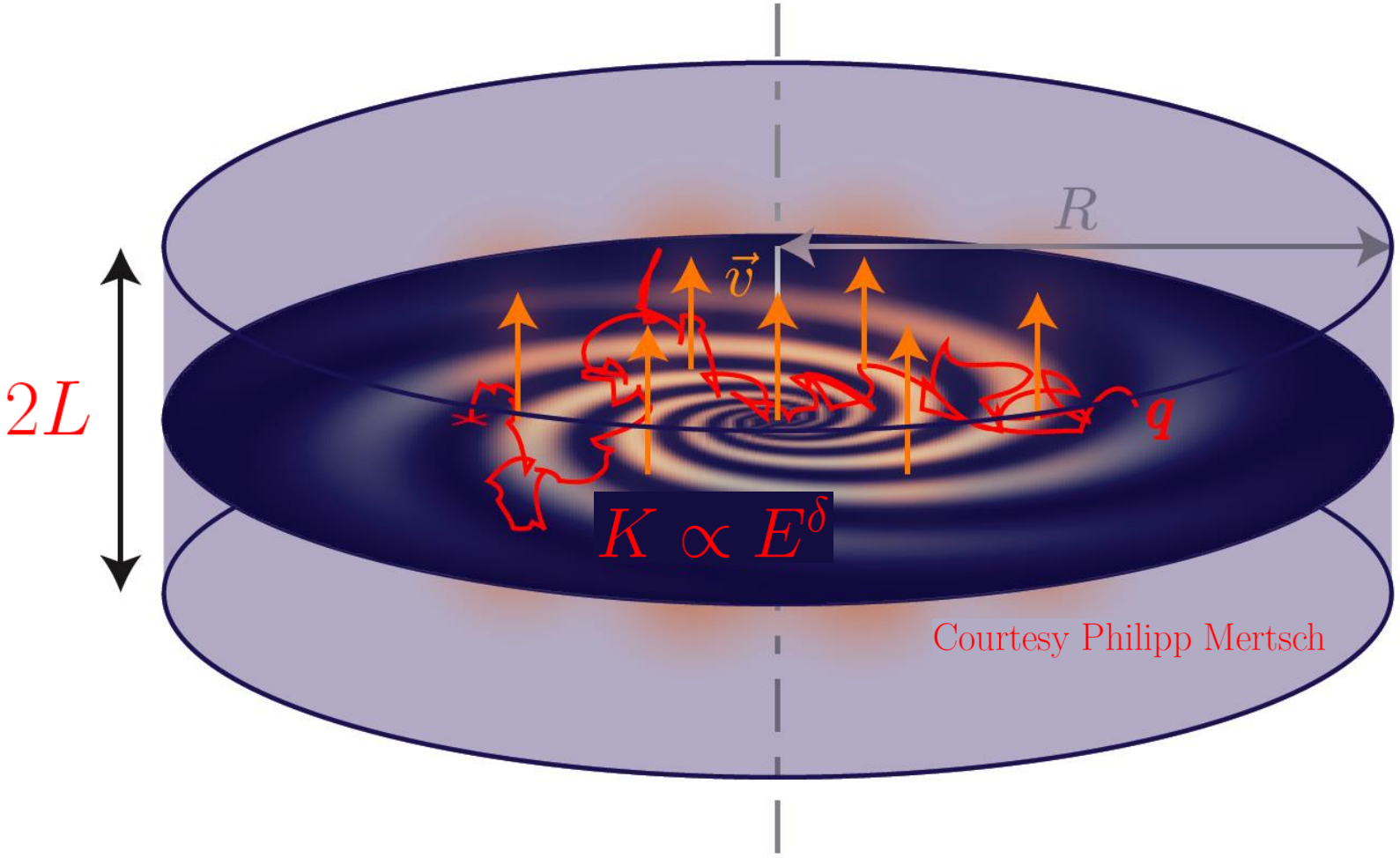

D. Maurin, R. Taillet, F. Donato, P. Salati, A. Barrau and G. Boudoul, *Galactic cosmic ray nuclei as a tool for astroparticle physics*, [astro-ph/0212111].

Cosmic–rays diffuse in space and energy

- A propagation model is characterized by the set δ, K_0, L, V_C, V_a

Case	δ	K_0 [kpc^2/Myr]	L [kpc]	V_C [km/s]	V_a [km/s]
max	0.46	0.0765	15	5	117.6
med	0.70	0.0112	4	12	52.9
min	0.85	0.0016	1	13.5	22.4

- Different methods to solve the CR diffusion equation

  The semi–analytic approach – radial Bessel expansion & Green functions

  The numerical Galprop code – Crank–Nicholson semi–implicit scheme

- Constraints from the typical secondary to primary B/C ratio

$$V_C \partial_z \Psi - K \Delta \Psi + \partial_E \left\{ b^{\rm loss}(E)\, \Psi - K_{EE}(E)\, \partial_E \Psi \right\} = Q$$

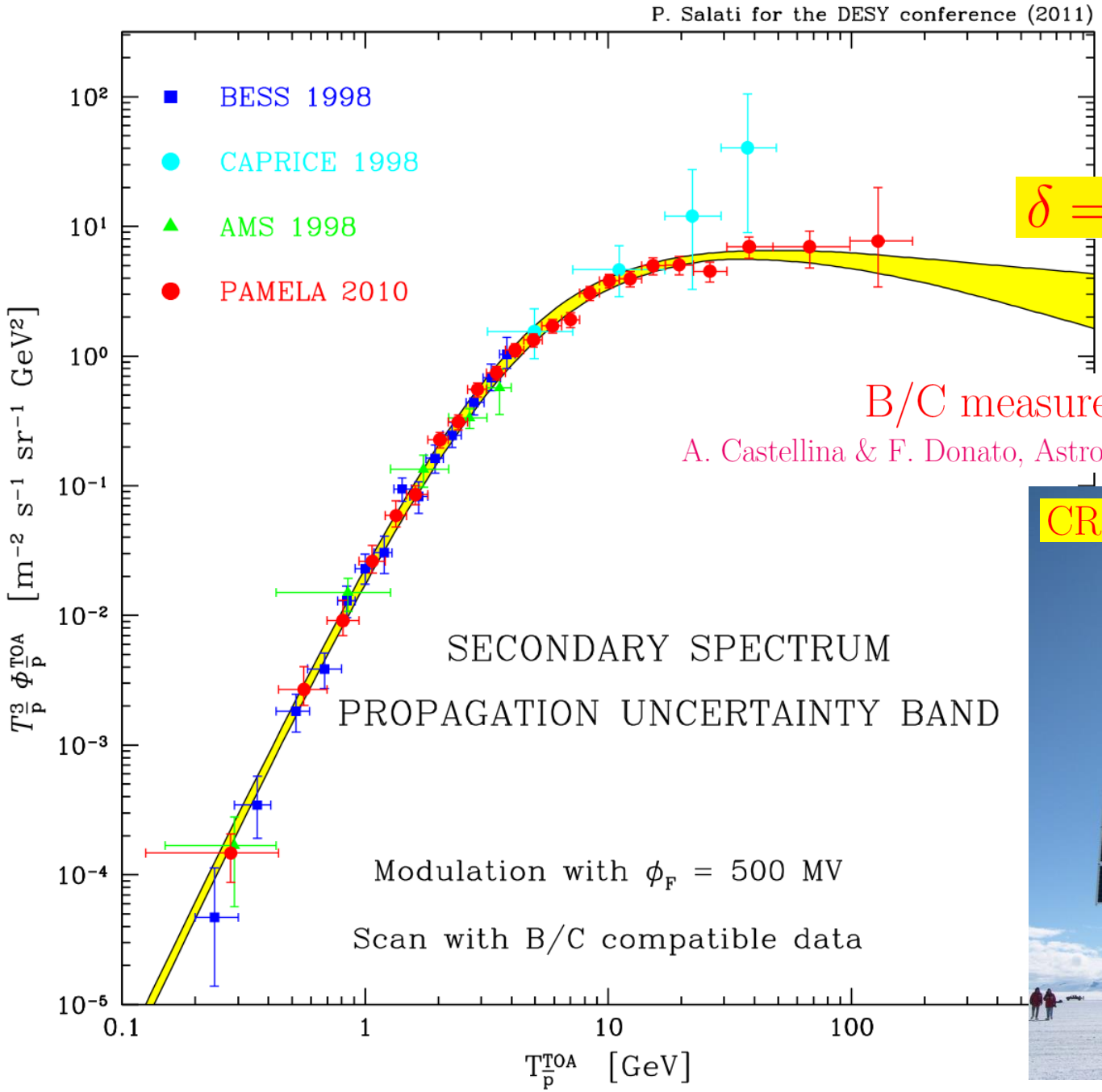

$\delta = 0.46$ to 0.85

B/C measurements @ high E

A. Castellina & F. Donato, Astropart. Phys. **24** (2005) 146-159

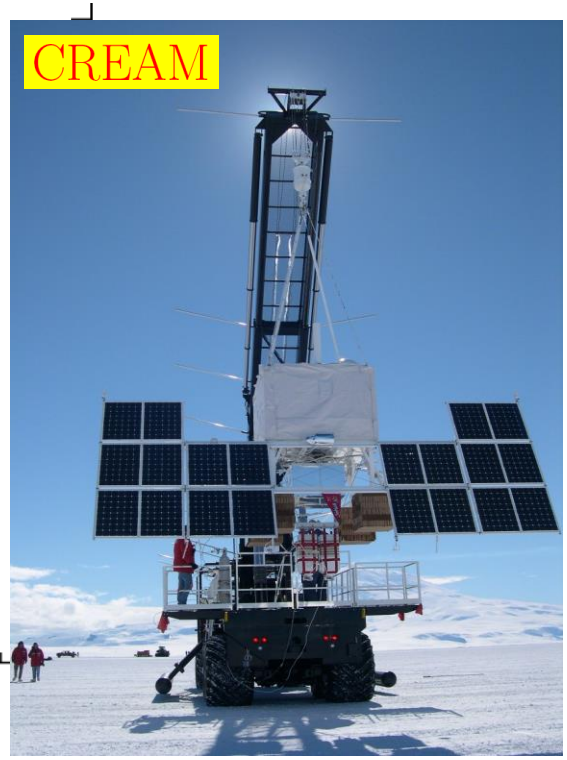

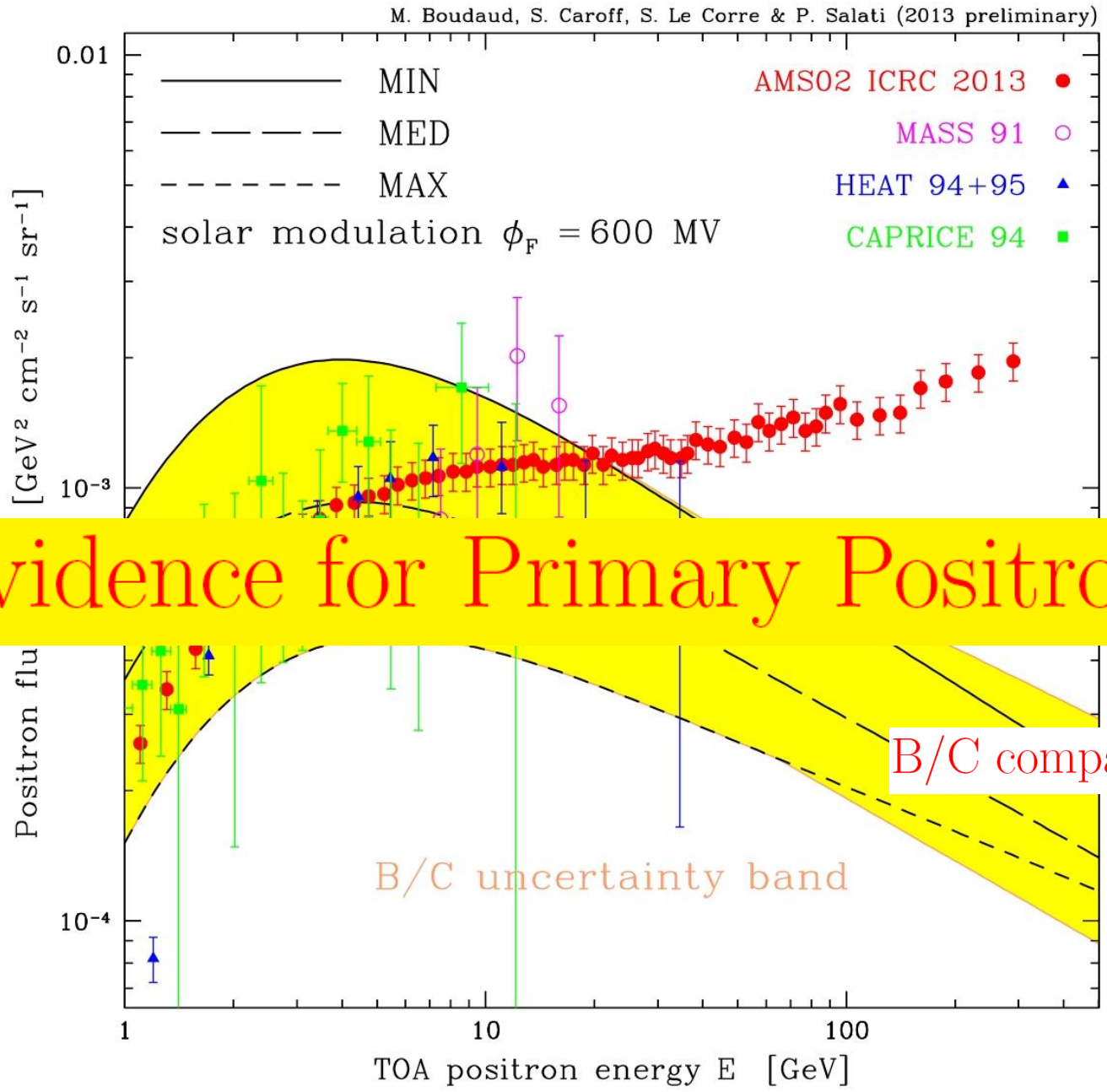

Evidence for Primary Positrons

MED model for CR retropropagation

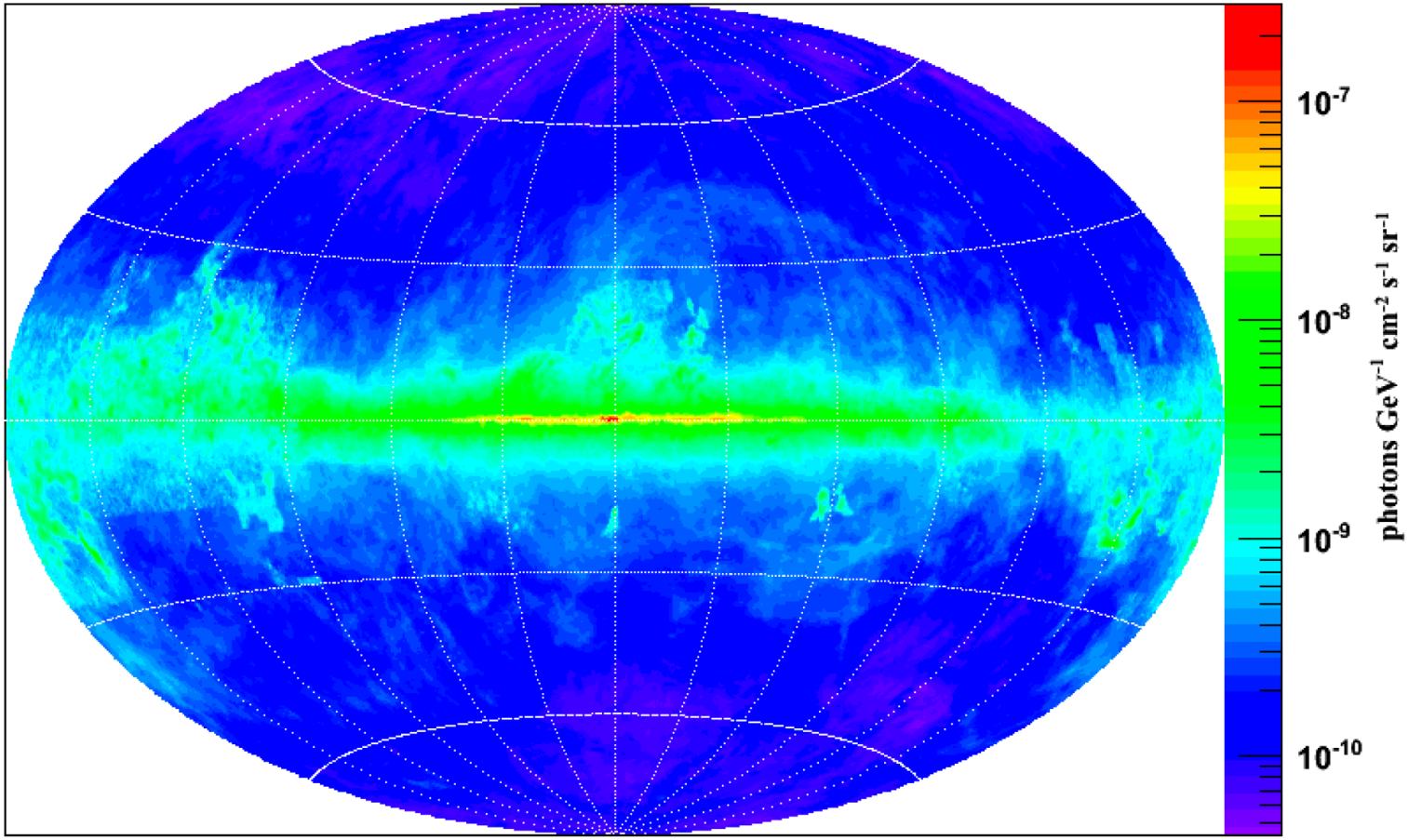

Fig. 1. Our reference map of the diffuse γ-ray emission of the Milky Way at 30 GeV obtained according to the method outlined in Sect. 2. The dominant hadronic component alone is considered. The cosmic ray proton and helium fluxes at the Earth's osition are taken from Shikaze et al. (2007). These fluxes were *retropropagated* throughout the DH with the Med model of Table 1. The distribution of primary CR sources in the Galactic disk was borrowed from Lorimer (2004). The differential photon production cross sections of CR protons and helium nuclei impinging on the ISM were parameterized according to Huang et al. (2007). This map is based on the HI and CO 3D Galactic distribution of Pohl et al. (2008). The $X_{\rm CO}$ factor was set equal to 2.3×10^{20} molecules cm^{-2} (K km s^{-1})$^{-1}$ everywhere in the Galaxy.

Uncer ;ation

Model	δ	K_0 [kpc^2/Myr]	L [kpc]	V_C [km/s]	V_a [km/s]
MIN	0.85	0.0016	1	13.5	22.4
MED	0.70	0.0112	4	12	52.9
MAX	0.46	0.0765	15	5	117.6

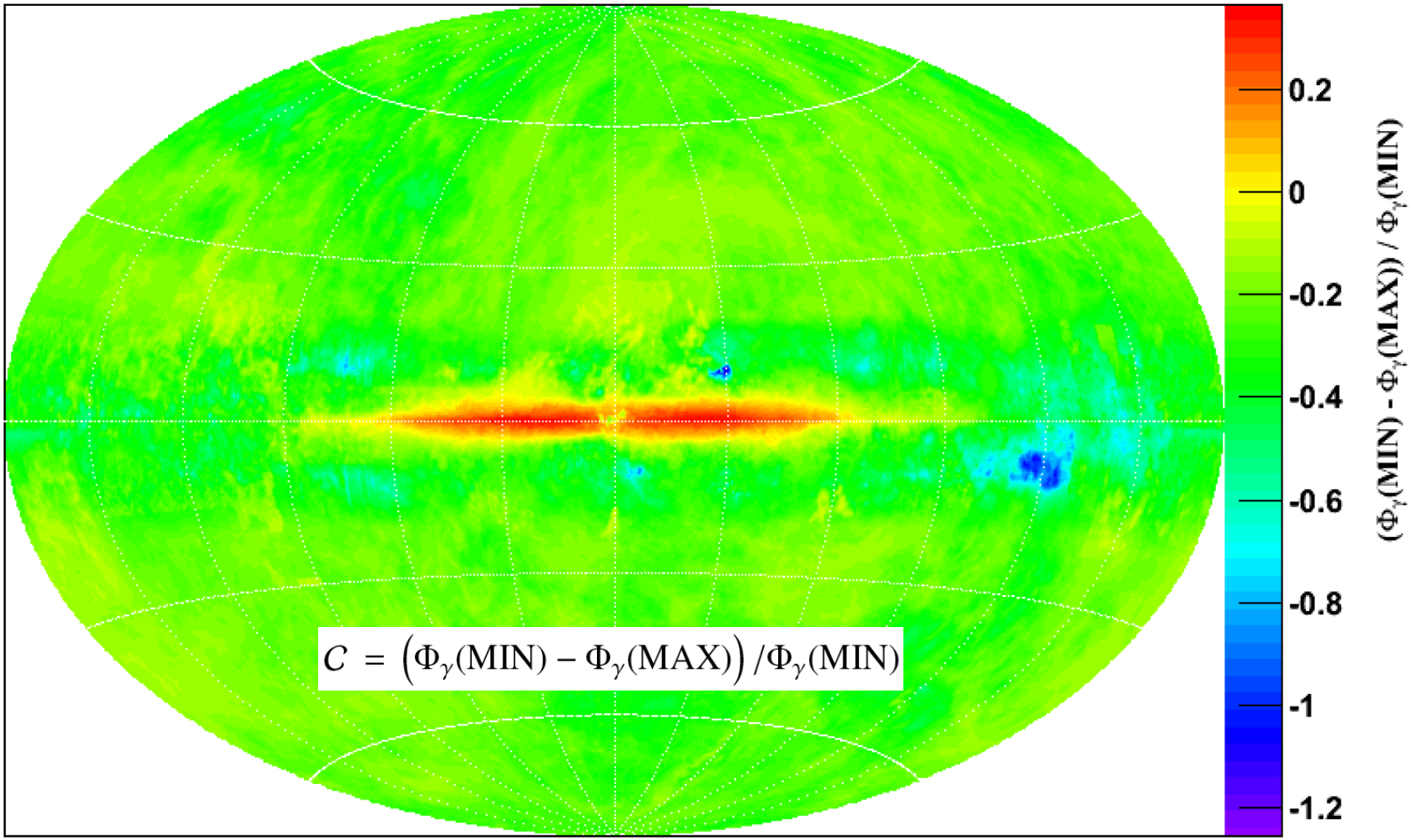

Fig. 2. This sky map features the difference between the MIN and MAX models relative to the MIN model. We have plotted for each pixel the ratio (map1 − map2)/map1 where map1 (map2) has been derived exactly like the γ-ray reference map of Fig. 1 with the sole difference of using the MIN (MAX) propagation parameters instead of the MED model.

2) The importance of multi–messenger analyses

• The degeneracy among the various CR propagation setups can be partially lifted if several observations are combined.

High–energy CR species & radio data

G. Di Bernardo, C. Evoli, D. Gaggero, D. Grasso & L. Maccione, JCAP **1303** (2013) 36

• The proton flux at the Earth and the B/C ratio provide informations on the primary CR nuclei injection spectrum at the sources.

$$D(\rho, R, z) = D_0 \ \beta^\eta f(z) \left(\frac{\rho}{\rho_0}\right)^\delta$$

$$D(z)^{-1} \propto B_{\rm ran}(z) \propto \exp\{-z/z_t\}$$

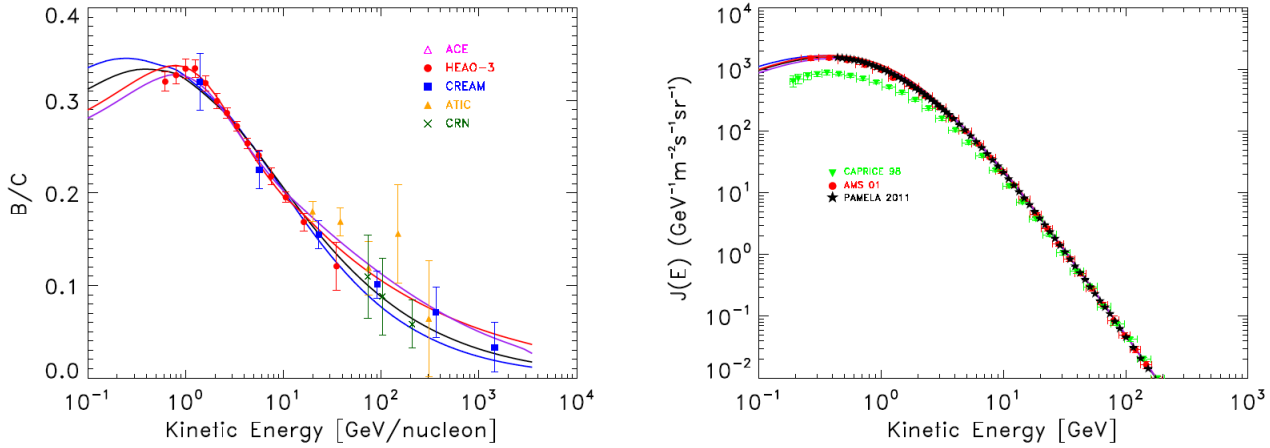

Figure 1. B/C and proton spectra computed for the reference propagation setups PD4 (black lines), KRA4 (blue) KOL4 (red) and CON4 (purple) defined in table 1 are compared with a selection of experimental data. The modulation potential used for the B/C is $\Phi = 0.5$ GV.

Model	D_0 (10^{28}cm^2/s)	v_A (km/s)	dV_c/dz (km/s/kpc)	δ	η	γ	Φ_p (GV)
PD8	3.64	0*	0*	0.56	-0.42	2.3	0.57
PD4	2.24	0*	0*	0.57	-0.40	2.29	0.56
PD2	1.11	0*	0*	0.58	-0.45	2.28	0.57
PD1	0.515	0*	0*	0.58	-0.40	2.29	0.58
KRA8	4.28	15.7	0*	0.5*	-0.39	2.35	0.68
KRA4	2.60	13.7	0*	0.5*	-0.39	2.36	0.65
KRA2	1.35	15.6	0*	0.5*	-0.41	2.35	0.67
KRA1	0.627	15.3	0*	0.5*	-0.40	2.33	0.69
KOL8	7.17	38.9	0*	0.33*	1*	2.00/2.40	0.52
KOL4	3.98	33.4	0*	0.33*	1*	1.93/2.47	0.51
KOL2	2.07	31.9	0*	0.33*	1*	1.91/2.47	0.54
KOL1	1.06	35.9	0*	0.33*	1*	1.81/2.40	0.47
CON8	0.952	36.1	50*	0.58	1*	1.92/2.48	0.52
CON4	0.923	36.0	50*	0.53	1*	1.94/2.48	0.52
CON2	0.794	34.5	50*	0.48	1*	1.95/2.46	0.52
CON1	0.573	31.4	50*	0.41	1*	1.95/2.46	0.52

Model	$\gamma_0(e^-)$	$\gamma(e^\pm)$	$E_{\rm cut}$ (GeV)	Φ (GV)	$\chi^2_{\rm FERMI}$
PD4	0.9/2.53	1.38	986	0.3	0.128
KRA4	0.6/2.53	1.50	967	0.3	0.20
KOL4	0.5/2.54	1.56	985	0.1	0.177
CON4	0.5/2.45	1.45	999	0.1	0.274

Table 2. We report here the source parameters which yield a consistent fit of the CRE and synchrotron spectra. The reported values of low energy spectral indexes are the maximum allowed to reproduce radio data at 2σ. The values of the force field modulation potential Φ have been fixed to match the e^- AMS-01 data. The reduced χ^2 is computed against the $e^+ + e^-$ spectrum and the positron fraction measured by Fermi-LAT.

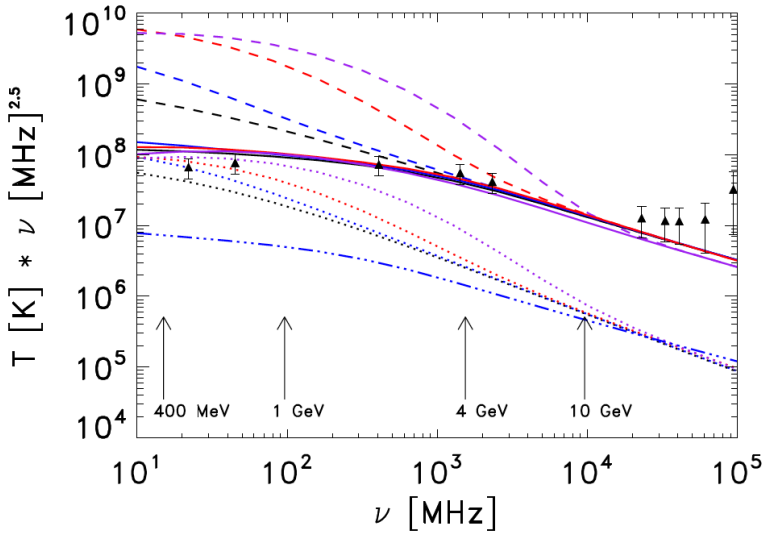

$$B_{\rm halo} = 4\ \mu{\rm G} \qquad\qquad B_{\rm ran}(0) = 7.6\ \mu{\rm G}$$

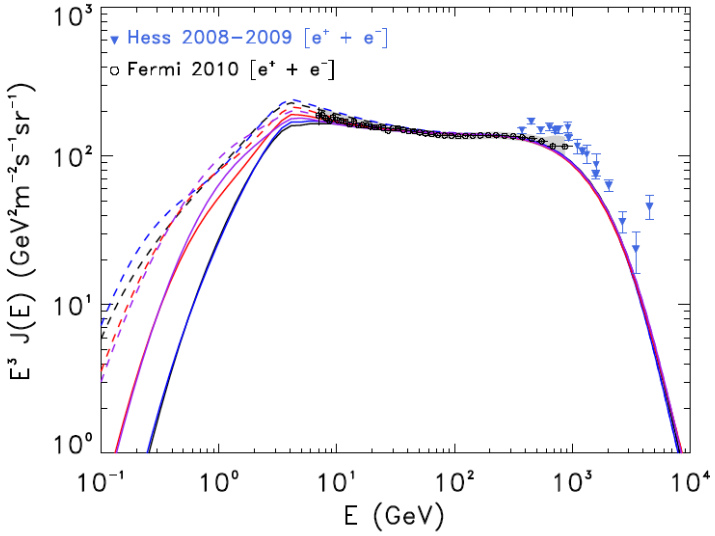
Hess 2008−2009 [e⁺ + e⁻]
Fermi 2010 [e⁺ + e⁻]
E³ J(E) (GeV²m⁻²s⁻¹sr⁻¹)
E (GeV)

(a)

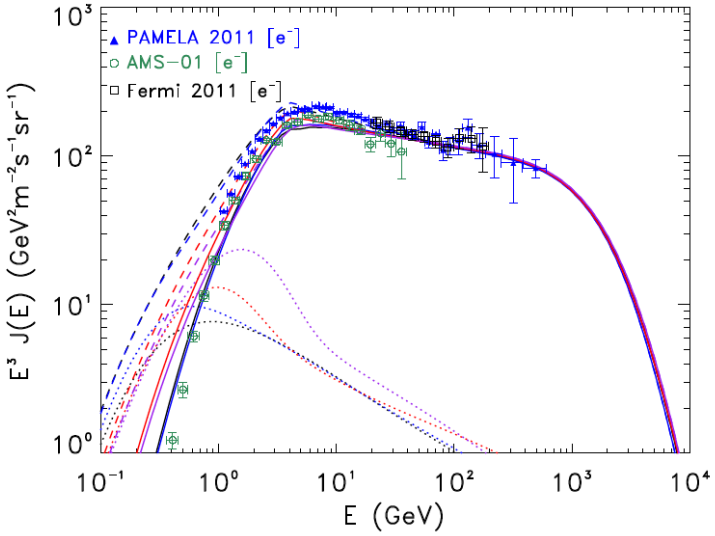
PAMELA 2011 [e⁻]
AMS−01 [e⁻]
Fermi 2011 [e⁻]
E³ J(E) (GeV²m⁻²s⁻¹sr⁻¹)
E (GeV)

(b)

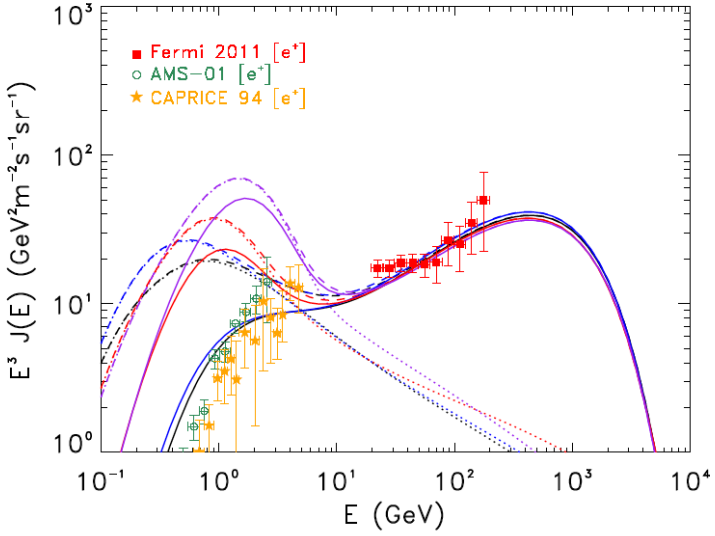
Fermi 2011 [e⁺]
AMS−01 [e⁺]
CAPRICE 94 [e⁺]
E³ J(E) (GeV²m⁻²s⁻¹sr⁻¹)
E (GeV)

(c)

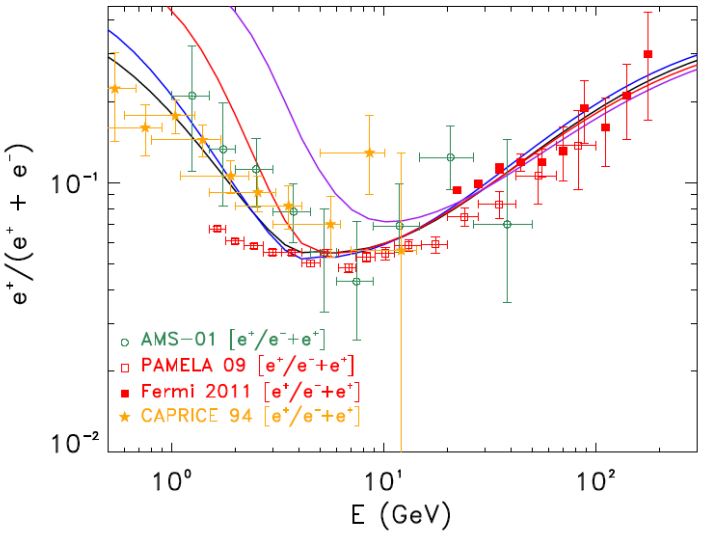
AMS−01 [e⁺/e⁻+e⁺]
PAMELA 09 [e⁺/e⁻+e⁺]
Fermi 2011 [e⁺/e⁻+e⁺]
CAPRICE 94 [e⁺/e⁻+e⁺]
e⁺/(e⁺ + e⁻)
E (GeV)

(d)

G. Di Bernardo, C. Evoli, D. Gaggero, D. Grasso & L. Maccione, JCAP **1303** (2013) 36

• The proton flux at the Earth and the B/C ratio provide informations on the primary CR nuclei injection spectrum at the sources.

• The injection of primary electrons by SNR and of an extra charge symmetric electron–positron component is constrained by

(i) Fermi–LAT data above 7 GeV

(ii) The average synchrotron spectrum for $40^\circ < l < 340^\circ$ and $10^\circ < |b| < 45^\circ$

• The electron and positron fluxes are **computed** below 7 GeV. Overproduction of secondary positrons in the KOL and CON models.

Diffusive reacceleration must be weak

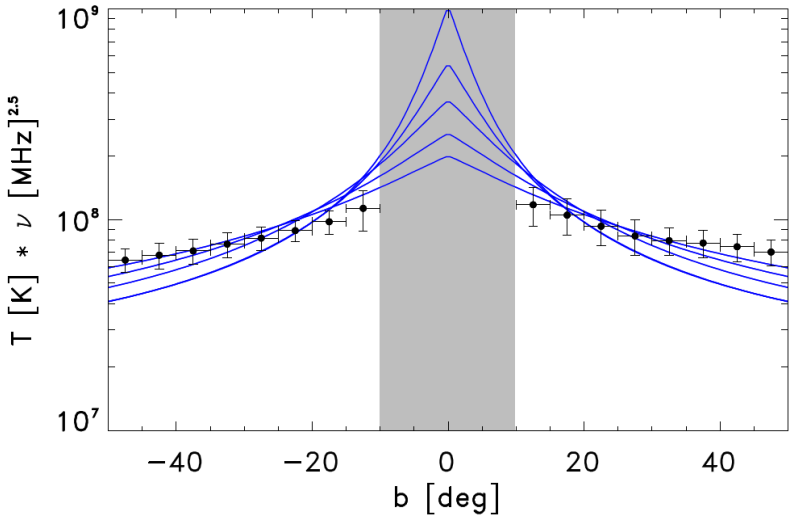

Figure 7. The latitude profiles of the synchrotron emission at 408 MHz in the region $40° < l < 100°$ computed for the KRA propagation setup and $z_t = 1, 2, 4, 8, 16$ kpc are compared with radio data. The grey shadowed region is not considered when placing the constraint.

z_t (kpc)	χ^2
1	2.7
2	2.5
4	1.6
8	0.9
16	0.4

G. Di Bernardo, C. Evoli, D. Gaggero, D. Grasso & L. Maccione, JCAP **1303** (2013) 36

• The proton flux at the Earth and the B/C ratio provide informations on the primary CR nuclei injection spectrum at the sources.

• The injection of primary electrons by SNR and of an extra charge symmetric electron–positron component is constrained by

(i) Fermi–LAT data above 7 GeV

(ii) The average synchrotron spectrum for $40^\circ < l < 340^\circ$ and $10^\circ < |b| < 45^\circ$

• The electron and positron fluxes are **computed** below 7 GeV. Overproduction of secondary positrons in the KOL and CON models.

Diffusive reacceleration must be weak

• The latitude profile of the synchrotron emission sets a limit on the magnetic halo scale height L which is sensitive to the vertical profile of $\mathbf{B}_{\rm ran}$.

$L \leq 2$ to 3 kpc

3) Magnetic turbulence & CR diffusion – a bubbling field

• Cosmic rays undergo pitch angle diffusion on the Alfvén waves – $\delta\mathbf{B}$ waves that propagate along the uniform component $\mathbf{B}_0$ and that are generated by the local plasma.

$$K(p) = \frac{1}{3} r_L(p)\, v(p)\, \frac{1}{k\, W(k)}\bigg|_{k=qB_0/pc} \qquad \text{while} \qquad \int_{k_0}^{\infty} dk\, W(k) = \frac{\delta B^2}{B_0^2}$$

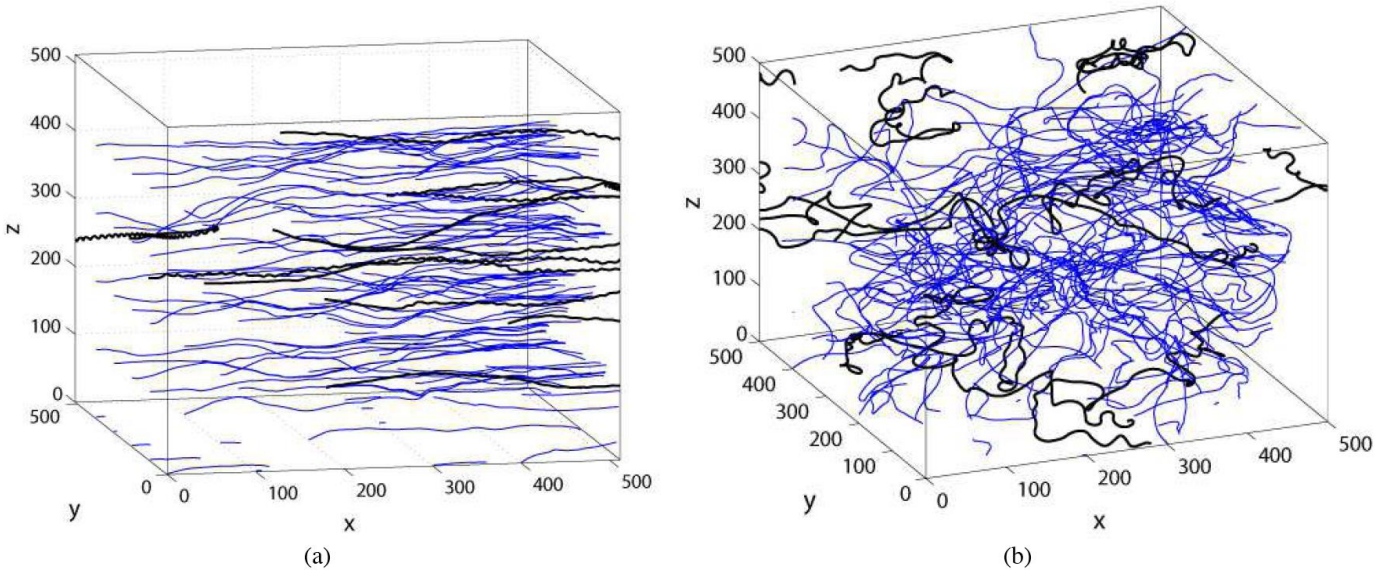

FIG. 1.— Particle trajectories (thick black lines) in (a) sub-Alfvénic turbulence with $M_A = 0.3$ and (b) super-Alfvénic turbulence with $M_A = 1.5$. The thin blue lines display the magnetic field stream lines.

SIYAO XU[1,2] AND HUIRONG YAN[1]

arXiv:1307.1346v2 [astro-ph.HE] 22 Jul 2013

3) Magnetic turbulence & CR diffusion – a bubbling field

• Cosmic rays undergo pitch angle diffusion on the Alfvén waves – $\delta\mathbf{B}$ waves that propagate along the uniform component $\mathbf{B}_0$ and that are generated by the local plasma.

$$K(p) = \frac{1}{3}\, r_L(p)\, v(p)\, \frac{1}{k\, W(k)}\bigg|_{k=qB_0/pc} \qquad \text{while} \qquad \int_{k_0}^{\infty} dk\, W(k) = \frac{\delta B^2}{B_0^2}$$

• Alfvén waves evolve in space and time according to MHD. They propagate with a velocity v_A in the plasma frame. MHD turbulence determines $W(k)$ – and eventually $K(p)$ – but the theory of turbulence is still in its infancy.

$$\frac{\partial}{\partial k}\left\{ D_{kk}\, \frac{\partial W}{\partial k} \right\} = q_W(k) \qquad \text{where} \qquad D_{kk} \propto v_A\, k^{7/2}\, W(k)^{1/2}$$

Sketch of Kolmogorov theory of turbulence

Courtesy Pasquale Serpico

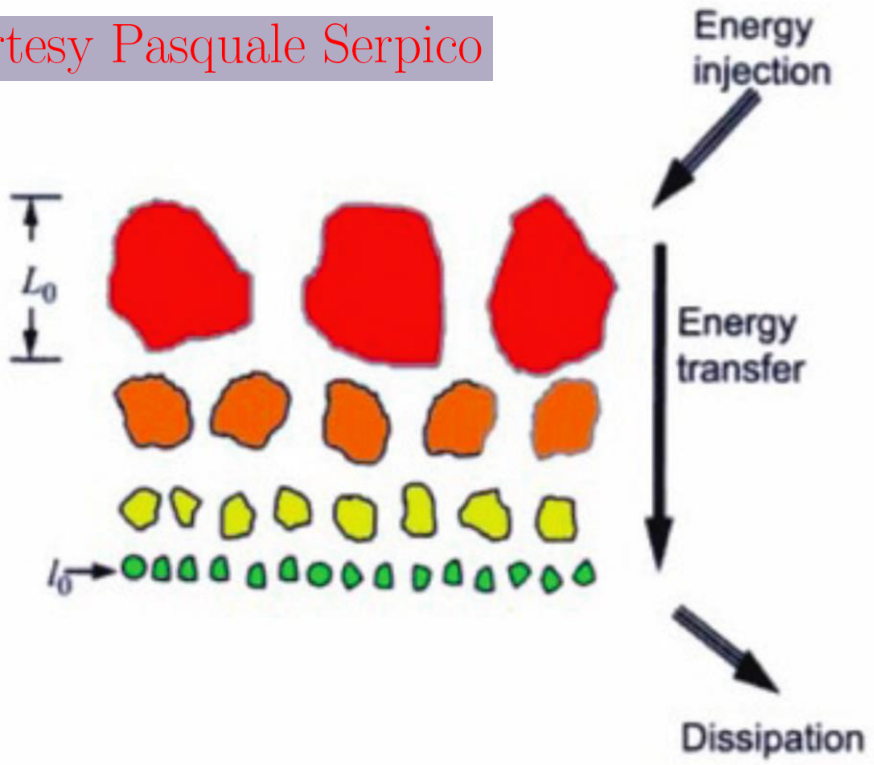

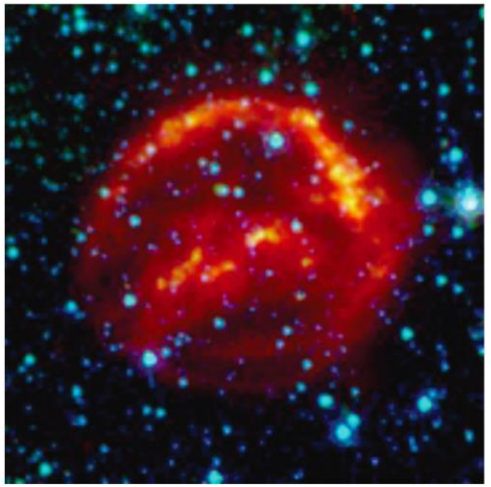

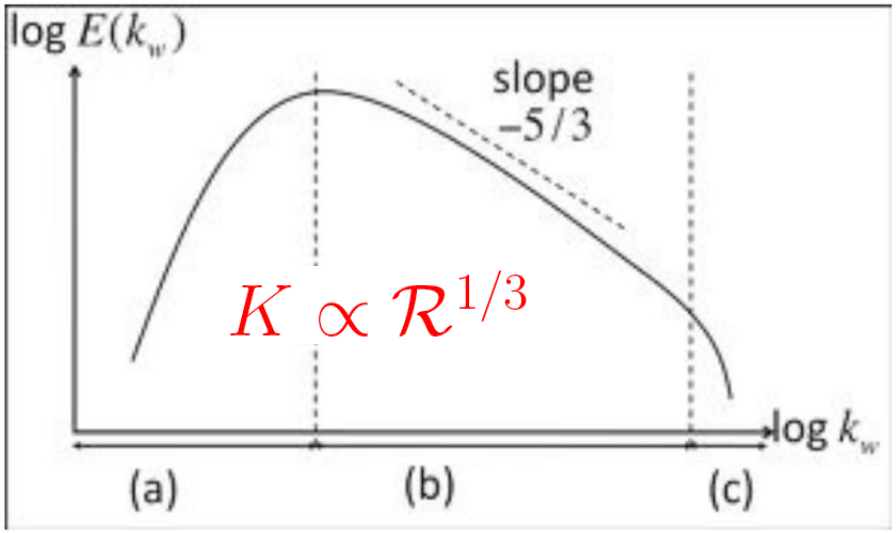

"External" power injected at large scale
e.g. SNRs at L_0~50 pc

Cascades down to dissipation scale
in a self-similar cascade

This constitutes the "inertial range" with
characteristic power-law

3) Magnetic turbulence & CR diffusion – a bubbling field

• Cosmic rays undergo pitch angle diffusion on the Alfvén waves – $\delta\mathbf{B}$ waves that propagate along the uniform component $\mathbf{B}_0$ and that are generated by the local plasma.

$$K(p) = \frac{1}{3}\, r_L(p)\, v(p)\, \frac{1}{k\, W(k)}\bigg|_{k=qB_0/pc} \qquad \text{while} \qquad \int_{k_0}^{\infty} dk\, W(k) \;=\; \frac{\delta B^2}{B_0^2}$$

• Alfvén waves evolve in space and time according to MHD. They propagate with a velocity v_A in the plasma frame. MHD turbulence determines $W(k)$ – and eventually $K(p)$ – but the theory of turbulence is still in its infancy.

$$\frac{\partial}{\partial k}\left\{ D_{kk}\, \frac{\partial W}{\partial k} \right\} = q_W(k) \qquad \text{where} \qquad D_{kk} \propto v_A\, k^{7/2}\, W(k)^{1/2}$$

• If the plasma is **advected** along the vertical direction and if a **vertical gradient** in CR density ψ is present, energy is transfered from the CR population to the Alfvén waves. The magnetic spectrum $W(k)$ is modified.

$$\frac{\partial}{\partial k}\left\{ D_{kk}\, \frac{\partial W}{\partial k} \right\} \;+\; \Gamma_{\rm CR}\, W = q_W(k)$$

Sketch of Kolmogorov theory of turbulence

Courtesy Pasquale Serpico

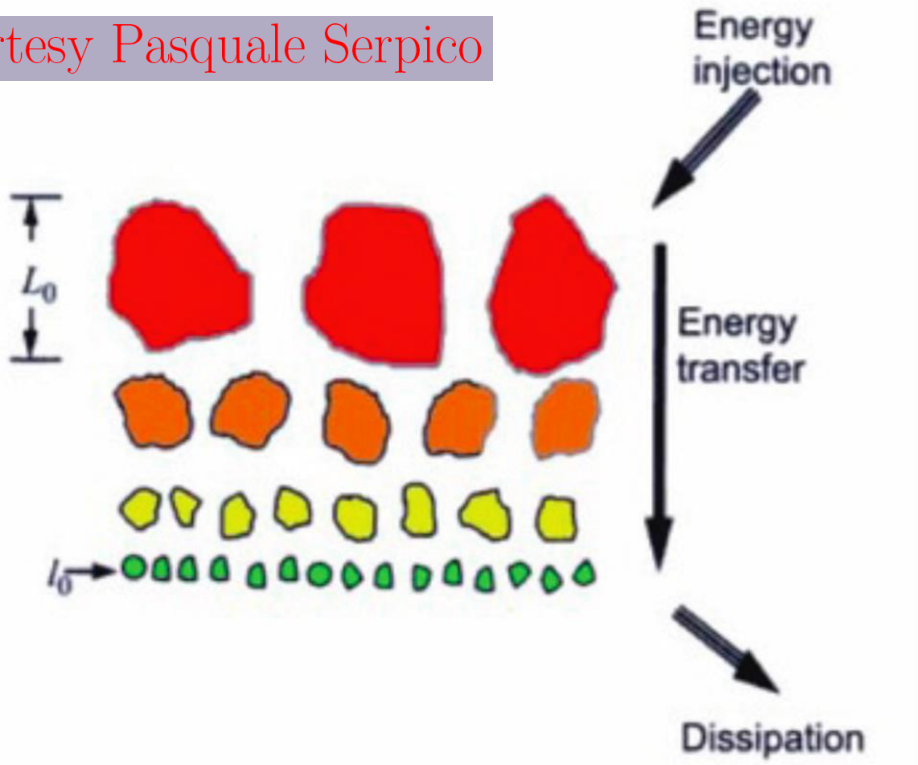

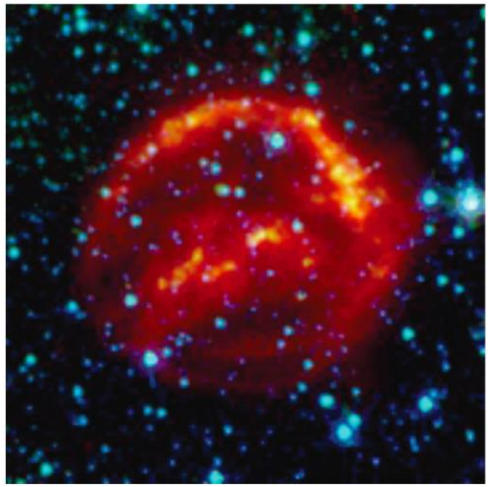

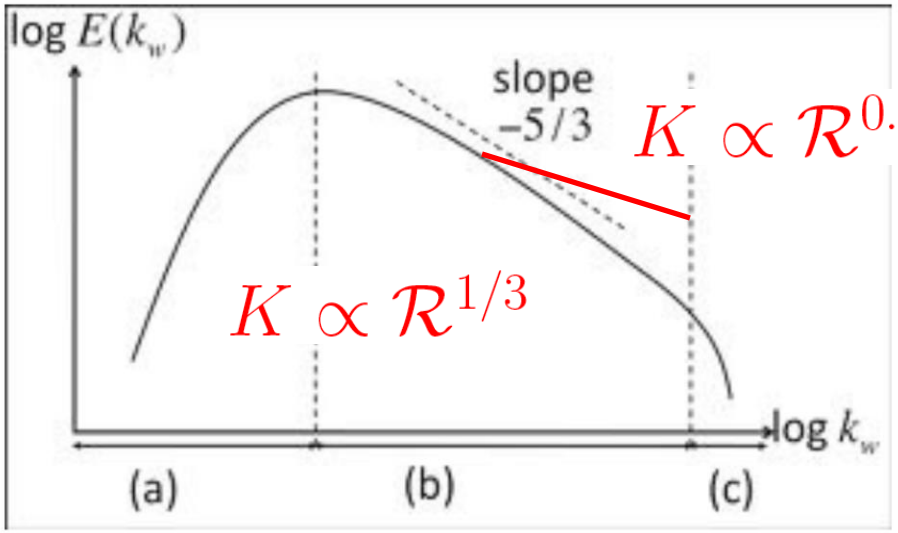

"External" power injected at large scale
e.g. SNRs at L_0~50 pc

Cascades down to dissipation scale
in a self-similar cascade

This constitutes the "inertial range" with
characteristic power-law

P. Blasi, E. Amato & P. Serpico, PRL **109** (2012) 061101

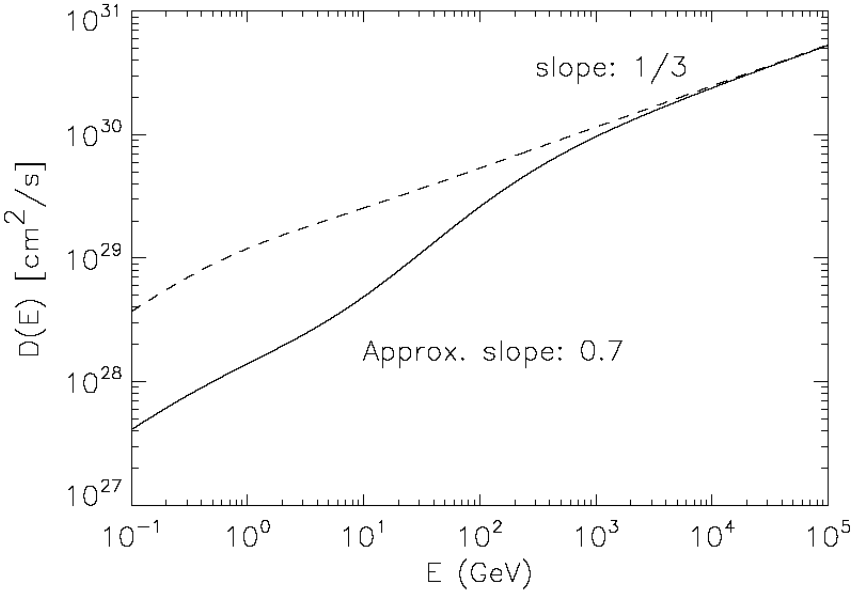

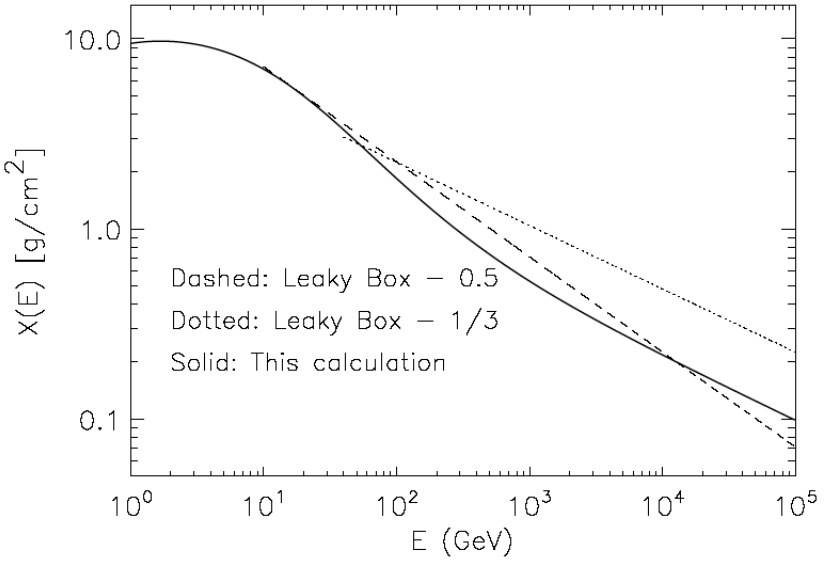

PAMELA Measurements of Cosmic-Ray Proton and Helium Spectra

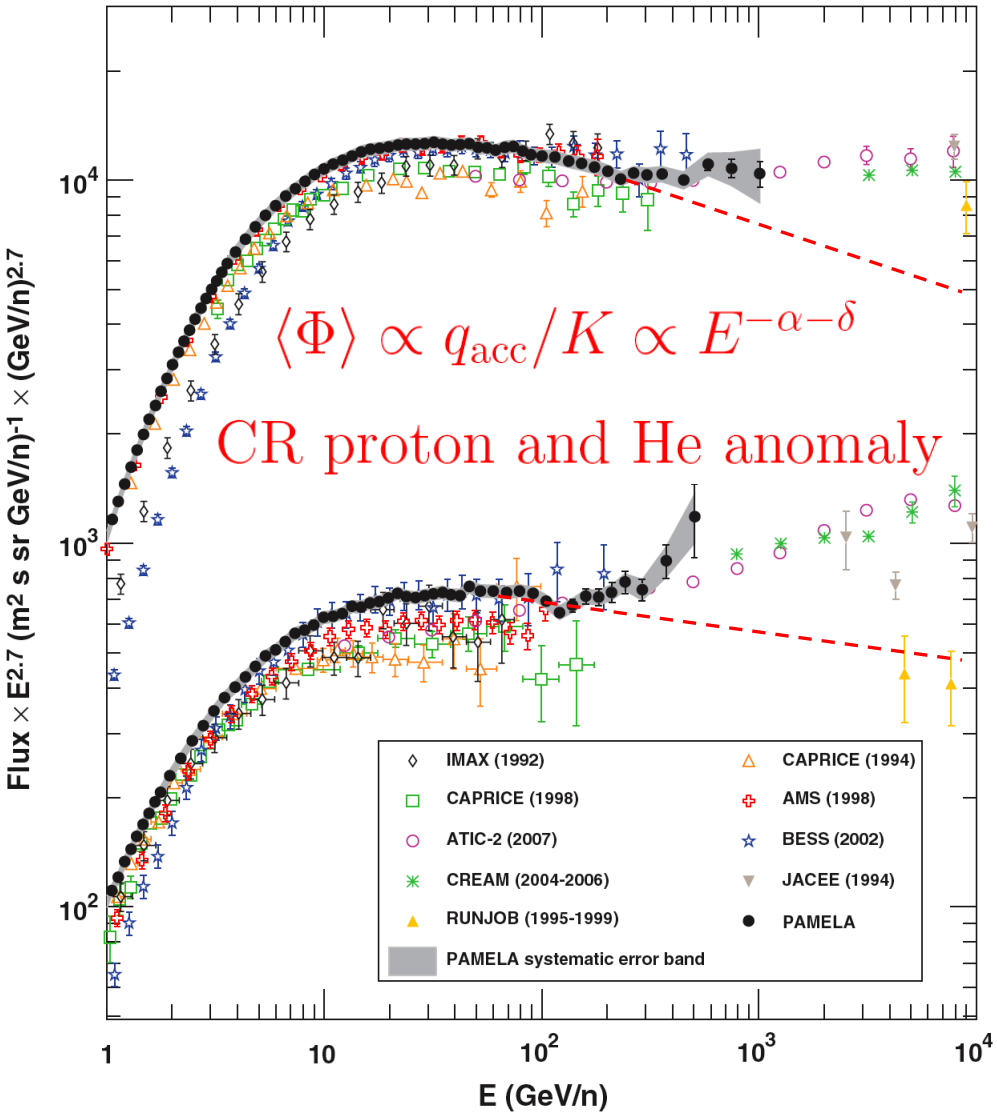

www.sciencemag.org **SCIENCE** VOL 332 1 APRIL 2011

4) Stochastic CR fluxes and the Myriad model

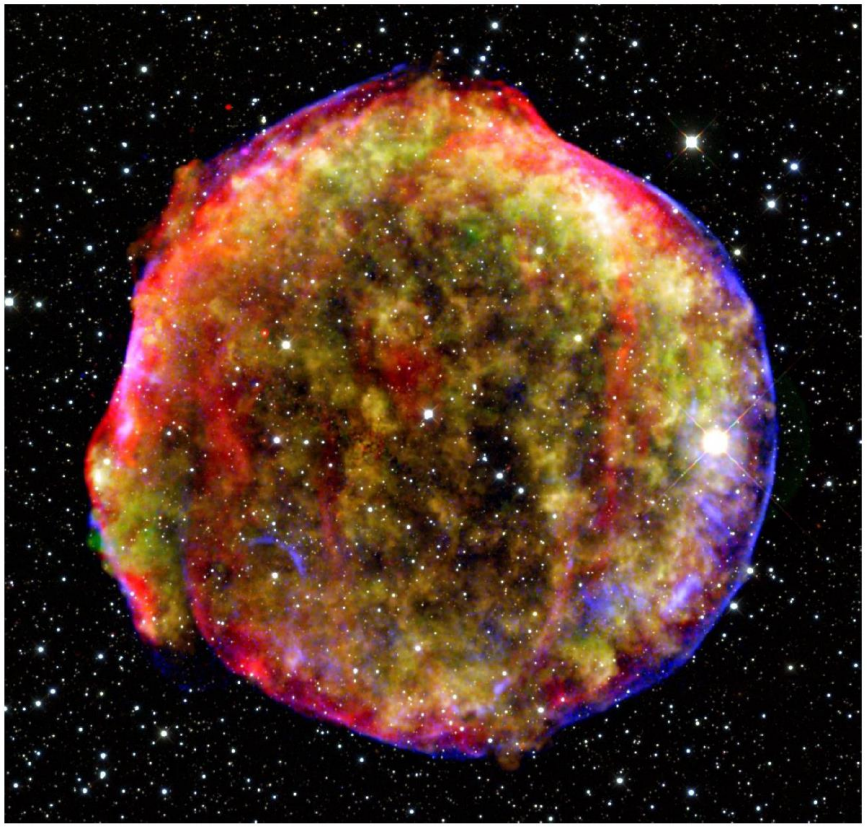

FIGURE 3.11: Restes de la SN de Tycho (1572)

• Supernova driven shock waves accelerate the elements of the interstellar medium through a first order Fermi mechanism. Nuclei and electrons are injected.

Observables

Stochastic time behaviour

Variations for discrete sources

Flux variations for Oxygen (Büsching et al. 2005)

10 GeV/nuc.

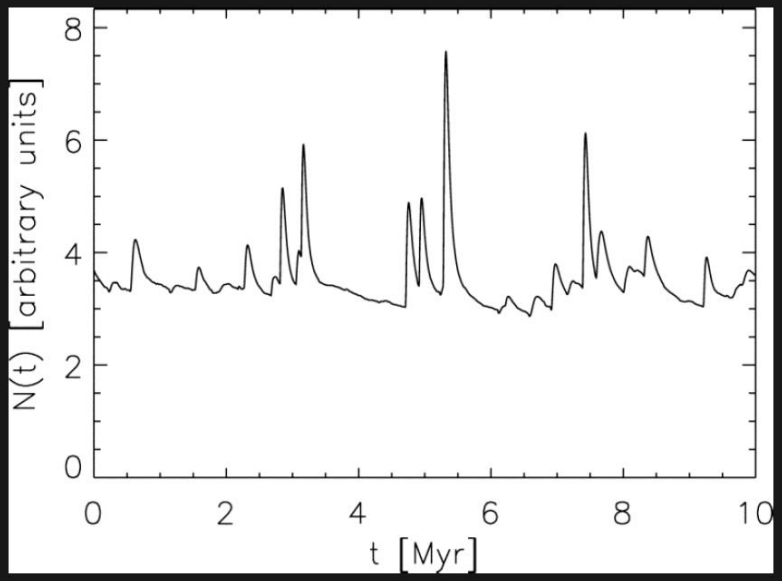

5 TeV/nuc.

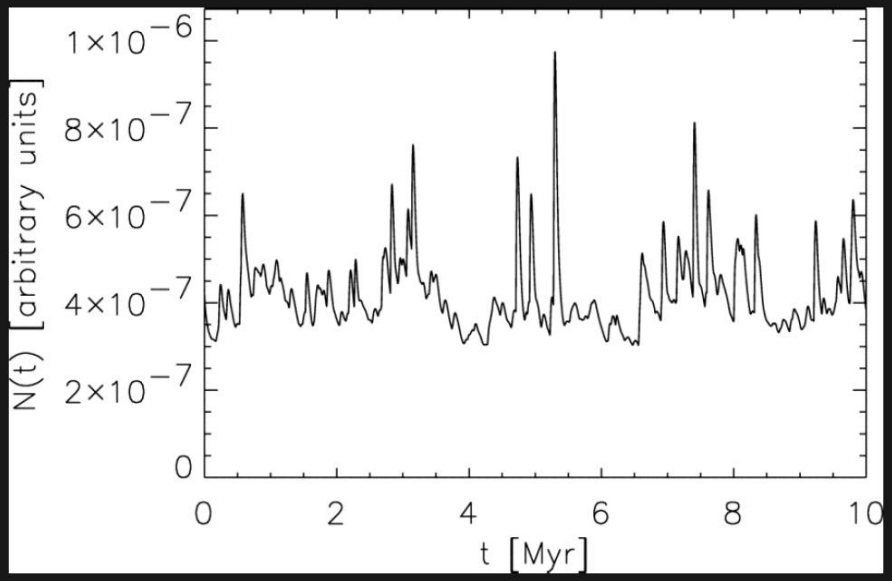

The Myriad model

• The sources of primary CR – supernova driven shock waves – are localized in space and time. They are discrete so that the total flux Φ of a given CR species is the sum over the population $\mathcal{P}$ of sources of the individual contributions φ_i

$$\Phi = \sum_{i \in \mathcal{P}} \varphi_i = \sum_{i \in \mathcal{P}} \frac{v_p}{4\pi} \times G_i \times q_{\rm SN}$$

• But we do **not** know where the sources are located and when they exploded.

A statistical analysis is mandatory

• This statistical analysis is carried out over the infinite set of the different possible populations of sources.

(i) Each source S is randomly distributed in space and time according to the probability distribution function $\mathcal{D}(\mathbf{x}_S, t_S)$. In particular, an explosion rate of $\nu \sim 1$ to 3 supernovae per century is assumed.

(ii) The $\mathcal{N}$ sources of any population are independent from each other – no correlation is assumed.

$$\langle \Phi \rangle = \sum_{i \in \mathcal{P}} \langle \varphi_i \rangle \equiv \mathcal{N} \times \langle \varphi \rangle$$

The average flux $\langle \Phi \rangle$ is **the same as in the standard CR model** where the sources behave as a continuous jelly with constant injection rate $q_{\rm acc} = \nu \times q_{\rm SN} \times \mathcal{D}(r_S)$.

• The variance of the flux gauges the possible spread of values arising from different populations $\mathcal{P}$.

$$\langle \Phi^2 \rangle - \langle \Phi \rangle^2 \equiv \sigma_\Phi^2 = \mathcal{N} \times \sigma_\varphi^2 \equiv \mathcal{N} \langle \varphi^2 \rangle - \frac{\langle \Phi \rangle^2}{\mathcal{N}}$$

In the limit where we go back at early times and take large values of the total number $\mathcal{N}$ of sources inside a given population $\mathcal{P}$, the variance simplifies into

$$\sigma_\Phi^2 = \mathcal{N} \times \langle \varphi^2 \rangle$$

which translates here into the integral

$$\sigma_\Phi = \frac{v_p}{4\pi} \times q_{\rm SN} \times \sqrt{\nu} \times \left\{ \int_{\mathcal{V}_{\rm tot}} G_p^2 \left(\mathbf{x}_\odot, t = 0 \leftarrow \mathbf{x}_S, t = t_S \right) \times \mathcal{D}(r_S) \times d^3 \mathbf{x}_S \, dt_S \right\}^{1/2}$$

• From a statistical point of view, **the standard CR model is correct if the variance σ_Φ is small**. Any population of sources would give in that case a flux Φ close to the average value $\langle \Phi \rangle$.

The calculation of σ_Φ is crucial !

calculation of σ_Φ

Statistical analysis on all possible populations of Galactic SN

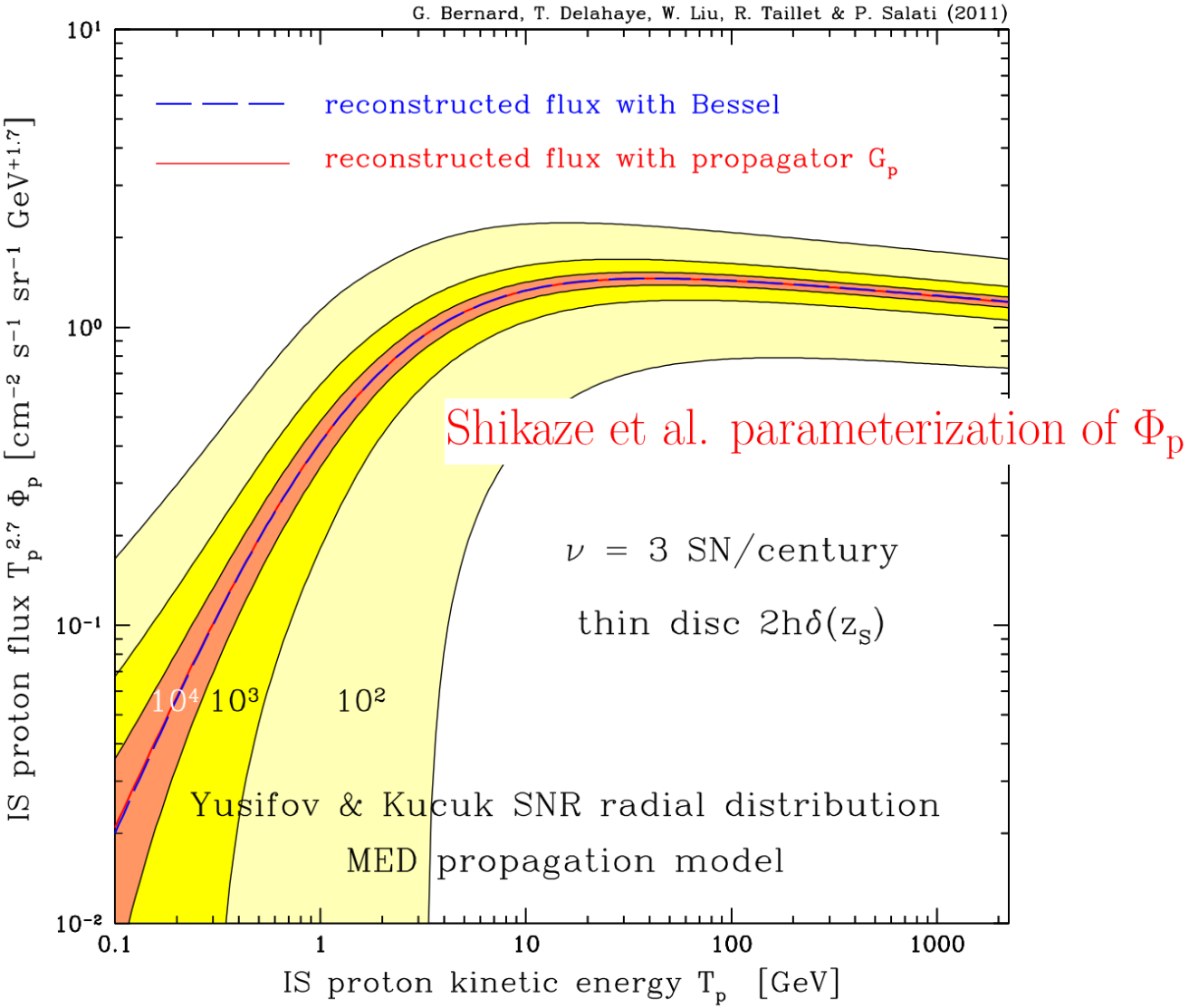

The variance σ_Φ is dominated by recent and local sources.

σ_Φ is infinite !

• An infinite variance is **terrible** because of the central limit theorem according to which the total CR proton flux should be distributed according to the Gaussian law

$$p\left(\langle\Phi\rangle\right) = \frac{1}{\sqrt{2\,\pi\,\sigma_\Phi^2}}\,\exp\left\{-\frac{\left(\Phi-\langle\Phi\rangle\right)^2}{2\,\sigma_\Phi^2}\right\}$$

• Several solutions have been suggested.

(i) We should merely give up the standard CR propagation model.

(ii) The variance σ_Φ can be regularized by setting for instance a limit on how close and young the sources are.

(iii) We should use a catalog for local and young sources and rely on the standard CR propagation model for the others.

The variance σ_Φ is dominated by recent and local sources.

σ_Φ is infinite !

- An infinite variance is **terrible** because of the central limit theorem according to which the total CR proton flux should be distributed according to the Gaussian law

$$p\left(\langle\Phi\rangle\right) = \frac{1}{\sqrt{2\,\pi\,\sigma_\Phi^2}}\,\exp\left\{-\frac{\left(\Phi-\langle\Phi\rangle\right)^2}{2\,\sigma_\Phi^2}\right\}$$

- Several solutions have been suggested.

(i) We should merely give up the standard CR propagation model.

(ii) The variance σ_Φ can be regularized by setting for instance a limit on how close and young the sources are.

(iii) We should use a catalog for local and young sources and rely on the standard CR propagation model for the others.

- We actually know the **near and recent sources**.

Table 1. Characteristics of nearby supernova remnants.

SNR G+long+lat	Other name	Distance [kpc]	Radio index σ_r	Brightness [Jy]	Age [kyr]	Pulsar
18.95−1.1		2. ± **0.1**	0.28	40	11.75 ± 0.85	?
65.3 + 5.7		0.9 ± 0.1	0.58 ± 0.07	52	26 ± **1**	∅
65.7 + 1.2	DA 495	1.0 ± 0.4	0.45 ± 0.1	5	16.75 ± 3.25	unknown
69.0 + 2.7	CTB 80	2.0 ± **0.1**	0.20 ± 0.10	60 ± 10	20 ± **1**	J1952 + 3252
74.0−8.5	Cygnus Loop	$0.54^{+0.10}_{-0.08}$	0.4 ± 0.06	175 ± 30	10 ± **1**	∅
78.2 + 2.1	γ Cygni	1.5 ± **0.1**	0.75 ± 0.03	275 ± 25	7 ± **1**	∅
82.2 + 5.3	W63	2.3 ± 1.0	0.36 ± 0.08	105 ± 10	20.1 ± 6.6	∅
89.0 + 4.7	HB 21	1.7 ± 0.5	0.27 ± 0.07	200 ± 15	5.60 ± 0.28	∅
93.7−0.2	CTB 104A / DA 551	1.5 ± 0.2	0.52 ± 0.12	42 ± 7	50 ± 20	∅
114.3 + 0.3		0.7	0.49 ± 0.25	6.4 ± 1.4	7.7 ± **0.1**	∅
116.5 + 1.1		1.6	0.16 ± 0.11	10.9 ± 1.2	20 ± 5	B2334 + 61?
116.9 + 0.2	CTB 1	1.6	0.33 ± 0.13	6.4 ± 1.4	20 ± 5	B2334 + 61?
119.5 + 10.2	CTA 1	1.4 ± 0.3	0.57 ± 0.06	42.5 ± 2.5	10 ± 5	J0010 + 7309
127.1 + 0.5	R5	1. ± 0.1	0.43 ± 0.1	12 ± 1	25 ± 5	∅
156.2 + 5.7		0.8 ± 0.5	$2.0^{+1.1}_{-0.7}$	4.2 ± 0.1	10 ± **1**	B0450 + 55?
160.9 + 2.6	HB 9	0.8 ± 0.4	0.48 ± 0.03	∼75	5.5 ± 1.5	B0458 + 46
180.0−1.7	S147	1.2 ± 0.4	0.75	74 ± 12	600 ± **10**	J0538 + 2817
184.6−5.8	Crab / 3C144 / SN1054	2.0 ± 0.5	0.3	1040	7.5 ⋆	B0521 + 31
189.1 + 3.0	IC 443	1.5 ± **0.1**	0.36 ± 0.04	160 ± 5	30 or 4	∅
203.0 + 12.0	Monogem ring	$0.288^{+0.033}_{-0.027}$			86 ± **1**	B0656 + 14
205.5 + 0.5	Monoceros nebula	1.63 ± 0.25	0.66 ± 0.2	156.1 ± 19.9	29 ± **1**	∅
263.9−3.3	Vela(XYZ)	0.295 ± 0.075	variable	2000 ± 700	11.2 ± **0.1**	B0833−45
266.2−1.2	Vela Jr / SN1300	0.75 ± **0.01**			3.5 ± 0.8 ⋆?	J0855−4644?
276.5 + 19.0	Antlia	0.2 ± 0.14			≥1000	B0950 + 08
315.1 + 2.7		1.7 ± 0.8	0.7		**50** ± **10**	J1423−56
330.0 + 15.0	Lupus Loop	0.8 ± 0.1			50 ± **10**	B1507−44?
347.3−0.5	SN393	1. ± 0.3			4.9 ⋆	∅
73.90 + 0.90		1.5 ± 0.5			11.5± 0.50	∅
107.50−1.50		1.1			4.5	∅
272.20−3.20		3.4 ± 1.6			8.5 ± 0.1	∅

Notes. Spectral index and brightness are inferred from measurements made at 1 GHz. Uncertainties in bold are not taken from bibliographic references, but just correspond to a rough uncertainty on the last relevant digit, so they can be underestimated. Age is flagged with a ⋆ for a historical remnant; in this case, the age uncertainty is set from the distance uncertainty. Except for the historical supernovæ, the ages are the *observed* ages, which differ from the *actual* ages by d/c.

TeV cosmic-ray proton and helium spectra in the myriad model

G. Bernard et al., A&A **555** (2013) A48

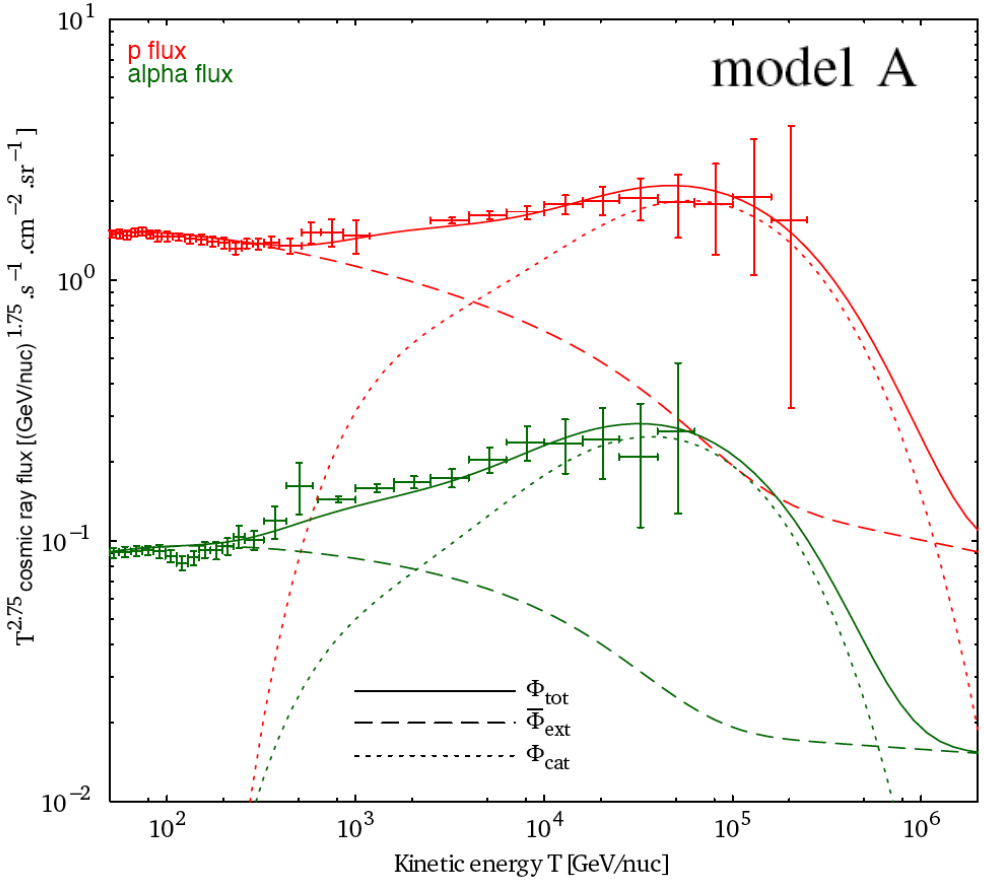

Model	K_0 [kpc^2/yr]	δ	L [kpc]	V_c [kpc/yr]	q_p^0 [GeV^{-1}]	q_{He}^0 [(GeV/n)$^{-1}$]
A	2.4×10^{-9}	0.85	1.5	1.38×10^{-8}	1.17×10^{52}	3.22×10^{51}
B	2.4×10^{-9}	0.85	1.5	1.38×10^{-8}	0.53×10^{52}	1.06×10^{51}
MED	1.12×10^{-9}	0.7	4	1.23×10^{-8}	15.8×10^{51}	3.14×10^{51}

model	$\alpha_p + \delta$	$\alpha_{He} + \delta$	ν [century^{-1}]	H injection	He injection	χ^2/d.o.f.
A	2.9	2.8	0.8	0.19	0.05	0.61
B	2.85	2.7	1.4	0.12	0.07	1.09
MED	2.85	2.7	0.8	0.148	0.07	1.3

The variance σ_Φ is dominated by recent and local sources.

σ_Φ is infinite !

- An infinite variance is **terrible** because of the central limit theorem according to which the total CR proton flux should be distributed according to the Gaussian law

$$p\left(\langle\Phi\rangle\right) = \frac{1}{\sqrt{2\,\pi\,\sigma_\Phi^2}}\,\exp\left\{-\frac{\left(\Phi-\langle\Phi\rangle\right)^2}{2\,\sigma_\Phi^2}\right\}$$

- Several solutions have been suggested.

(i) We should merely give up the standard CR propagation model.

(ii) The variance σ_Φ can be regularized by setting for instance a limit on how close and young the sources are.

(iii) We should use a catalog for local and young sources and rely on the standard CR propagation model for the others.

(iv) The variance of the flux is infinite but this is not a problem because the PDF does exist.

3) The generalized central limit theorem

Courtesy Philipp Mertsch

- The variance of the flux is infinite but this is not a problem.

The PDF of the total flux Φ **does exist**

It can be determined by running a Monte-Carlo simulation over the various populations of CR sources.

G. Bernard, T. Delahaye, P. Salati & R. Taillet, A&A **544** (2012) A92

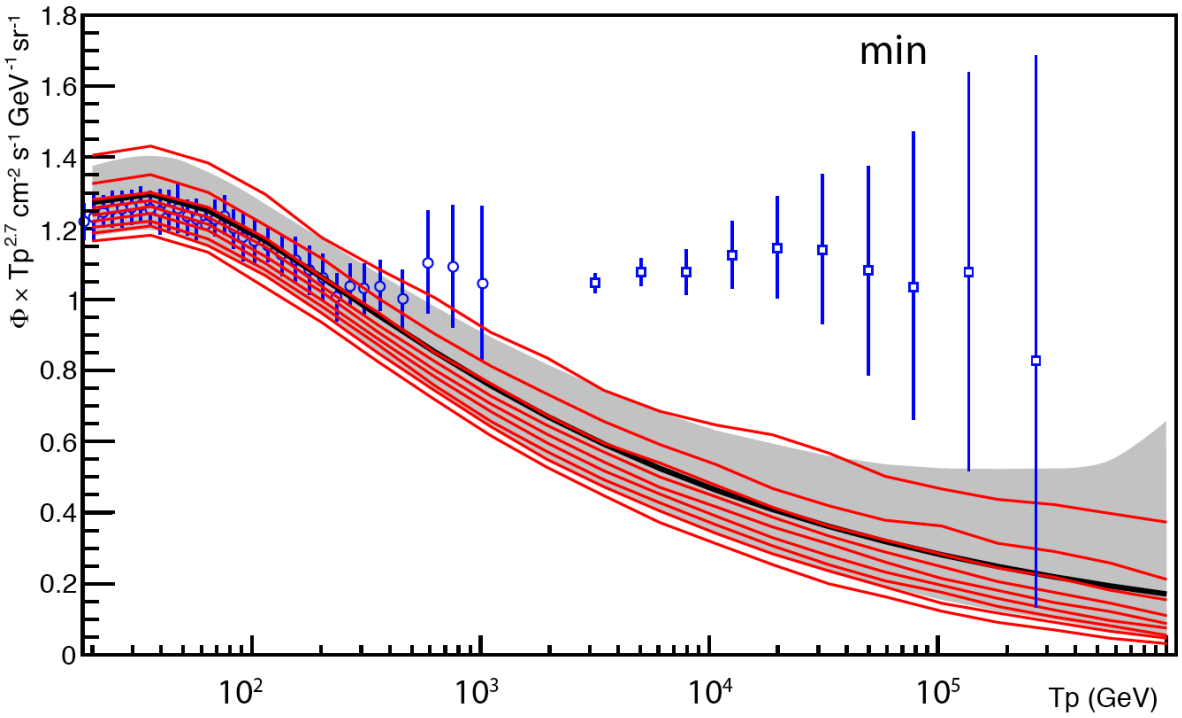

• The probability distribution function (PDF) of the flux φ from an individual source is related to its distribution in space and time through

$$dP \,=\, p(\varphi)\, d\varphi \,=\, \int_{\mathcal{V}_\varphi} \mathcal{D}(\mathbf{x}_S, t_S)\; d^3\mathbf{x}_S\; dt_S$$

In the limit where the flux is large, the propagation boils down to diffusion in 3D space with

$$\varphi \,=\, \frac{v_p}{4\pi} \times q_{\rm SN} \times \frac{1}{(4\pi K\tau)^{3/2}}\; e^{-r^2/4K\tau} \,=\, \frac{a}{\tau^{3/2}}\; e^{-r^2/4K\tau}$$

• The probability that the flux is larger than some value φ is called **the survival function** $R(\varphi)$ and may be expressed as

$$R(\varphi) \,=\, \int_{\varphi}^{+\infty} dP \,=\, \int_0^{\tau_{\rm M}} d\tau\; \frac{4\pi}{3}\, r_\tau^3\; \mathcal{D}(\mathbf{x}_\odot, 0)$$

where the maximal age $\tau_{\rm M}$ is defined as

$$\varphi \,=\, \frac{a}{\tau_{\rm M}^{3/2}}$$

Sources with age $\tau \leq \tau_{\rm M}$ yield a flux larger than φ inside a sphere whose radius r_τ is defined as

$$r_\tau^2 \,=\, 6K\tau_{\rm M} \times (-x \ln x) \text{ where } x = \tau/\tau_{\rm M}$$

- The survival function $R(\varphi)$ behaves as $\varphi^{-5/3}$ in the large flux limit where

$$\lim_{\varphi \to +\infty} \varphi^{5/3}\, R(\varphi) \;=\; \pi^{3/2}\, (2/5)^{5/2}\, \mathcal{D}(\mathbf{x}_\odot, 0)\, (6K)^{3/2}\, a^{5/3} \;\equiv\; c$$

- The variance is infinite because $p(\varphi) \propto \varphi^{-8/3}$ when the flux is large. This is not a problem since the PDF of the total flux Φ does exist.

$$\frac{(\Phi - \langle \Phi \rangle)}{\Sigma_\Phi} \text{ is distributed according to } \mathrm{S}(5/3, 1, 1, 0; 1)$$

- The spread of the total flux Φ is gauged by

$$\Sigma_\Phi \;=\; \left\{ \frac{\pi\, \mathcal{N}\, c}{2\, \Gamma(5/3)\, \sin(5\pi/6)} \right\}^{3/5} \;\propto\; q_{\mathrm{SN}} \times K^{-3/5} \times \nu^{3/5}$$

The relative spread of the total flux Φ behaves as

- $\dfrac{\Sigma_\Phi}{\langle \Phi \rangle} \;\propto\; V_C \times K^{-3/5} \times \nu^{-2/5}$ at low energy
- $\dfrac{\Sigma_\Phi}{\langle \Phi \rangle} \;\propto\; L^{-1} \times K^{2/5} \times \nu^{-2/5}$ at high energy

Model A - L = 1.5 kpc

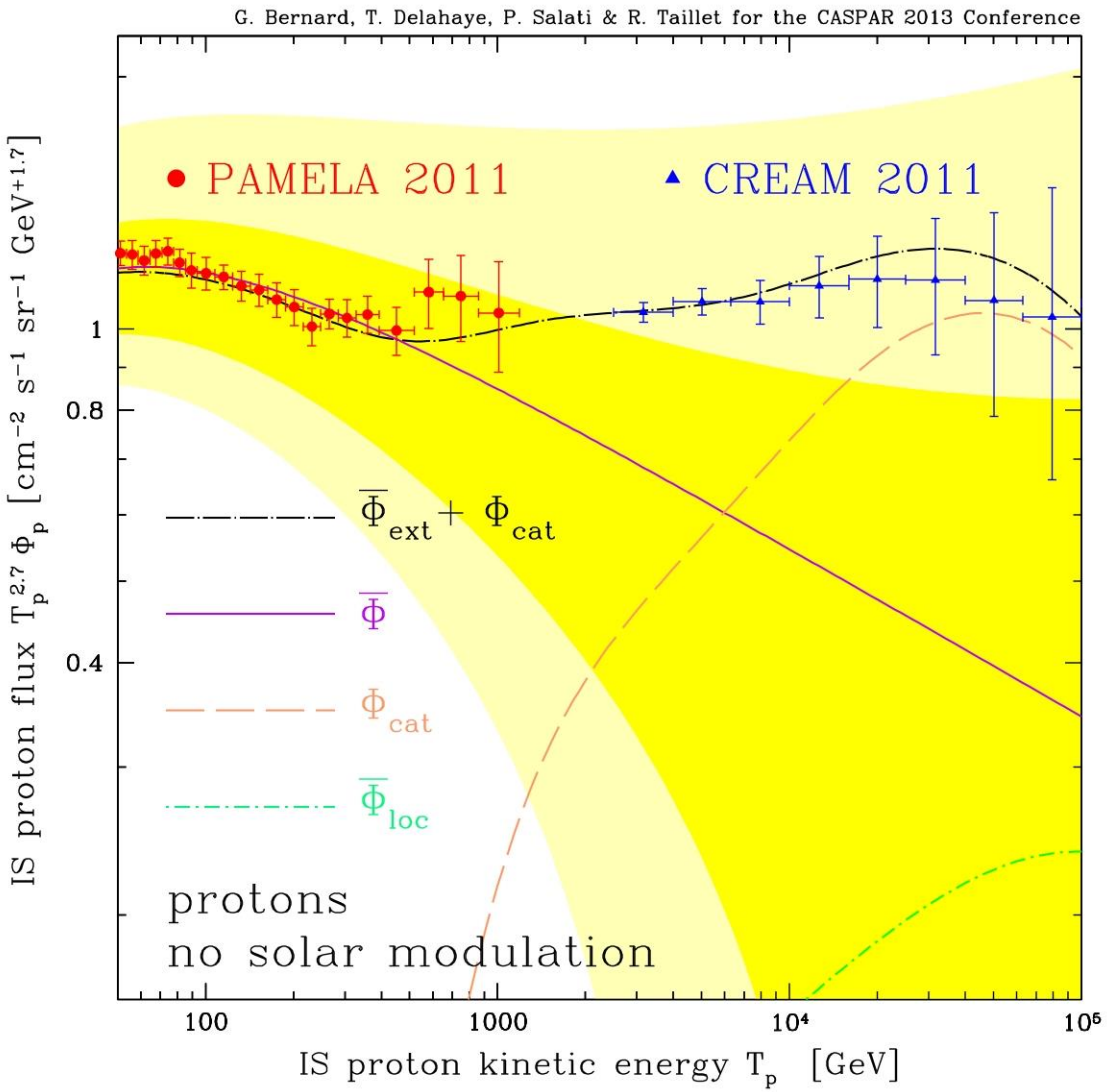

Model A - L = 1.5 kpc - Gaussian PDF

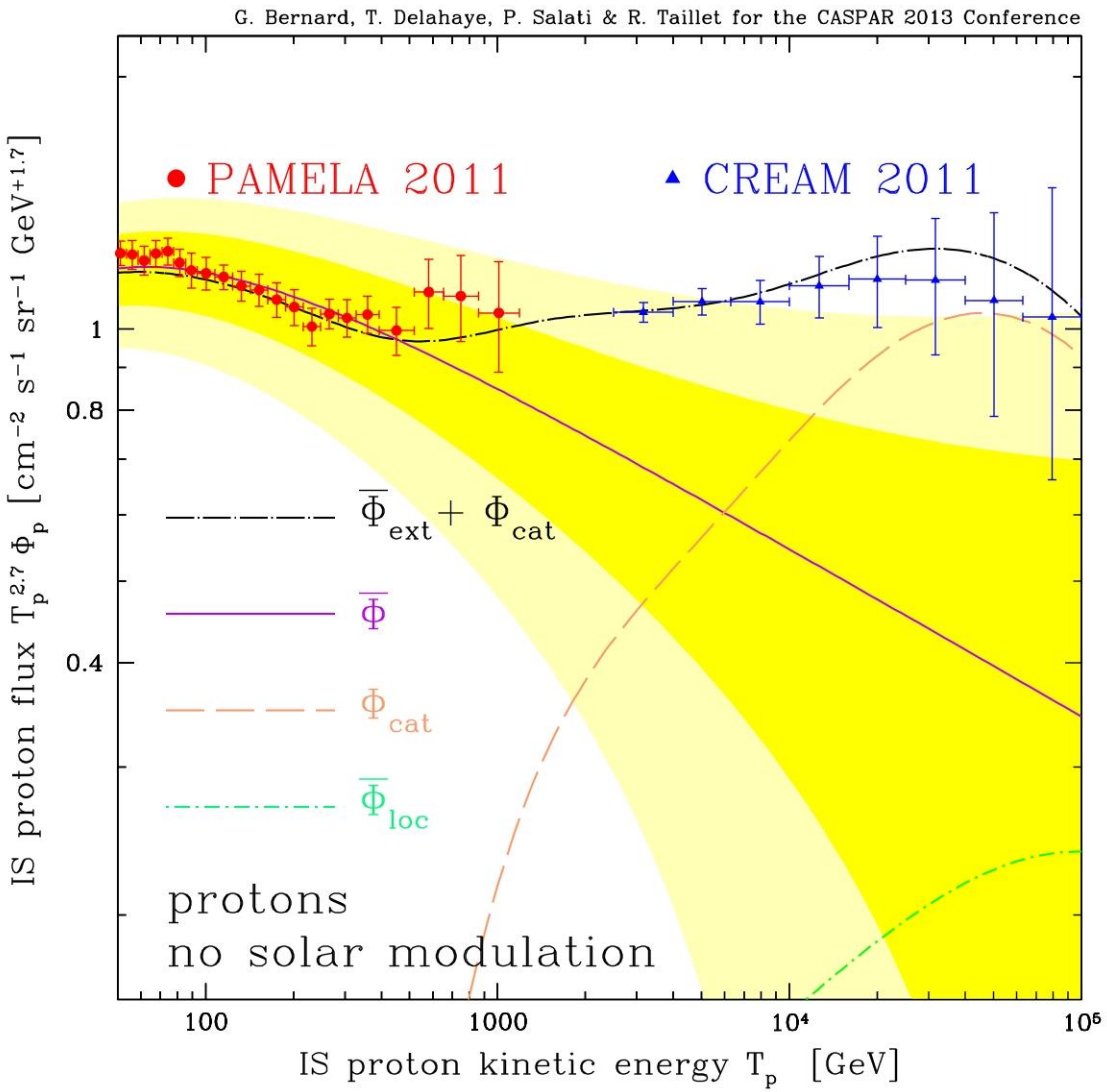

Conclusions and perspectives

• As the precision of the observations has increased, life has become harder.

✓ The propagation parameters of the simplest CR propagation model need to be determined with a multi–messenger analysis including charged CR, gamma ray and radio data.

✓ Refined models may be used to interpret observations like 3D codes. **But extracting the uncertainties on CR propagation may be more difficult than for simple models.**

• One way to remedy this problem is to use MHD in order to **predict** CR propagation parameters.

• The discreteness of the sources – neglected in the past – should be taken into account in order to bridge the physics of the sources with what is observed on larger scales.

✓ The generalized central limit theorem provides an efficient tool – competitive with MC analyses – to gauge the corresponding uncertainty. Stochastic fluctuations are expected to be small at low energy and when L is large.

✓ An excess of the primary CR proton & helium spectra becomes pathological – i.e., stops to be a mere fluctuation – when L is large. If so, explaining the PAMELA & CREAM anomalies with local sources is no longer tenable.

✓ The next step is to investigate the problem of anisotropies. MC analyses may not be the ultimate tool because of heavy tails in the PDF.

Microphysics of propagation & source discreteness

The next challenge

2) The importance of multi–messenger analyses

• The degeneracy among the various CR propagation setups can be partially lifted if several observations are combined.

High–energy CR species & radio data

• Primary electrons are injected by SNR with a spectral index α of 2.5–2.7. This is too steep to be compatible with DSA for which α is 2.2–2.4. A 3D code can remedy that problem.

• The primary electron injection spectrum is harder if a catalog of nearby SNR and pulsars is used.

T. Delahaye, J. Lavalle, R. Lineros, F. Donato & N. Fornengo, A&A **524** (2010) A51

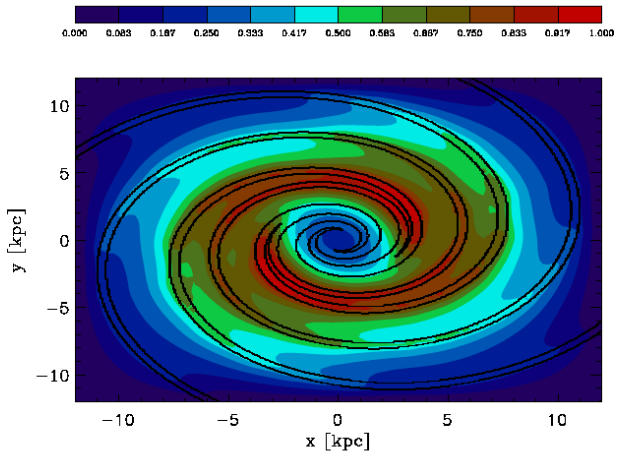

Fig. 3: CR electron distribution on the Galactic plane at 1 GeV.

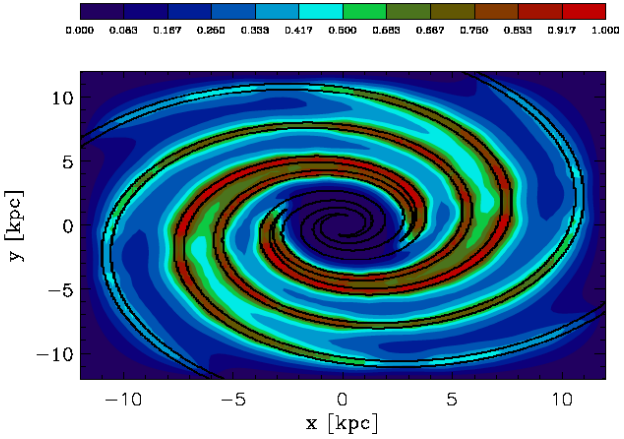

Fig. 4: CR electron distribution on the Galactic plane at 100 GeV.

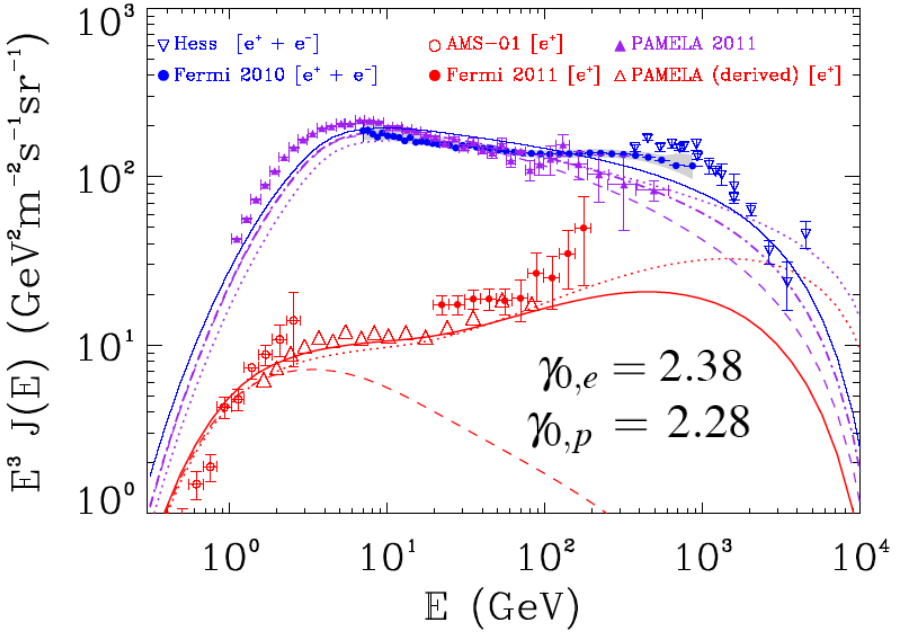

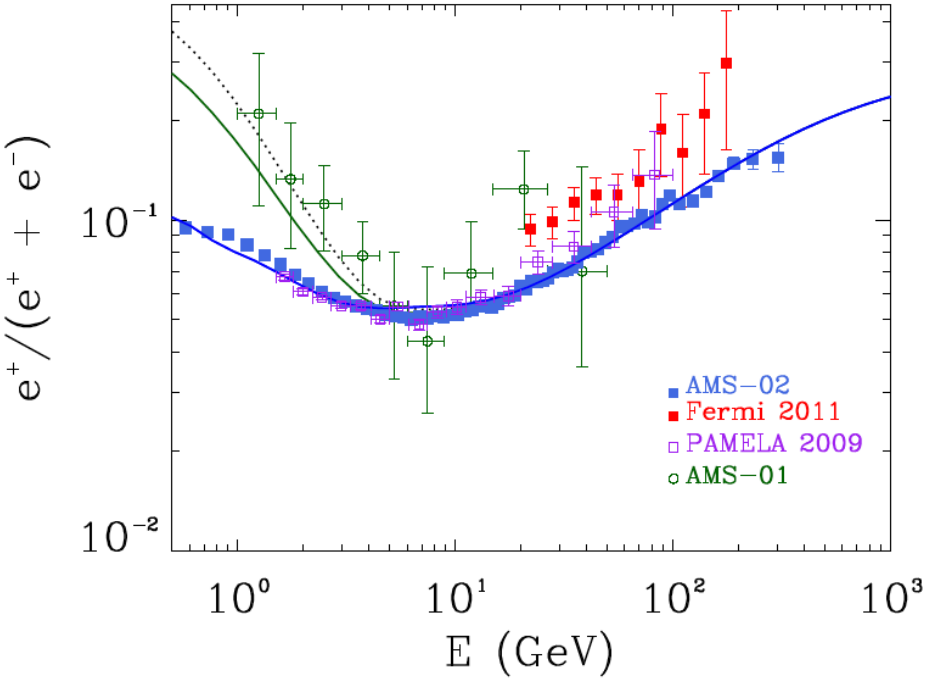

2) The importance of multi–messenger analyses

• The degeneracy among the various CR propagation setups can be partially lifted if several observations are combined.

High–energy CR species & radio data

• Primary electrons are injected by SNR with a spectral index α of 2.5–2.7. This is too steep to be compatible with DSA for which α is 2.2–2.4. A 3D code can remedy that problem.

• The primary electron injection spectrum is harder if a catalog of nearby SNR and pulsars is used.

T. Delahaye, J. Lavalle, R. Lineros, F. Donato & N. Fornengo, A&A **524** (2010) A51

	L04 SNRs	local SNRs (Green)	local SNRs (ATNF)	L04 pulsars	local pulsars (ATNF)
Spectral index	2.4	†	2.4	2.0	2.0
$\widetilde{\Gamma}_E$ [10^{48} erg/100 yr]	21	$6 \times$ †	from $B(1\,\mathrm{GHz}) = 1\,\mathrm{Jy}$	3.6×10^{-2}	†
Converted fraction [%]	-	-	-	-	0.6
E_c [TeV]	2.0	2.0	2.0	1.5	1.5

Andrii Neronov & Dmitri Semikoz – CASPAR 2013
Stochastic space behaviour

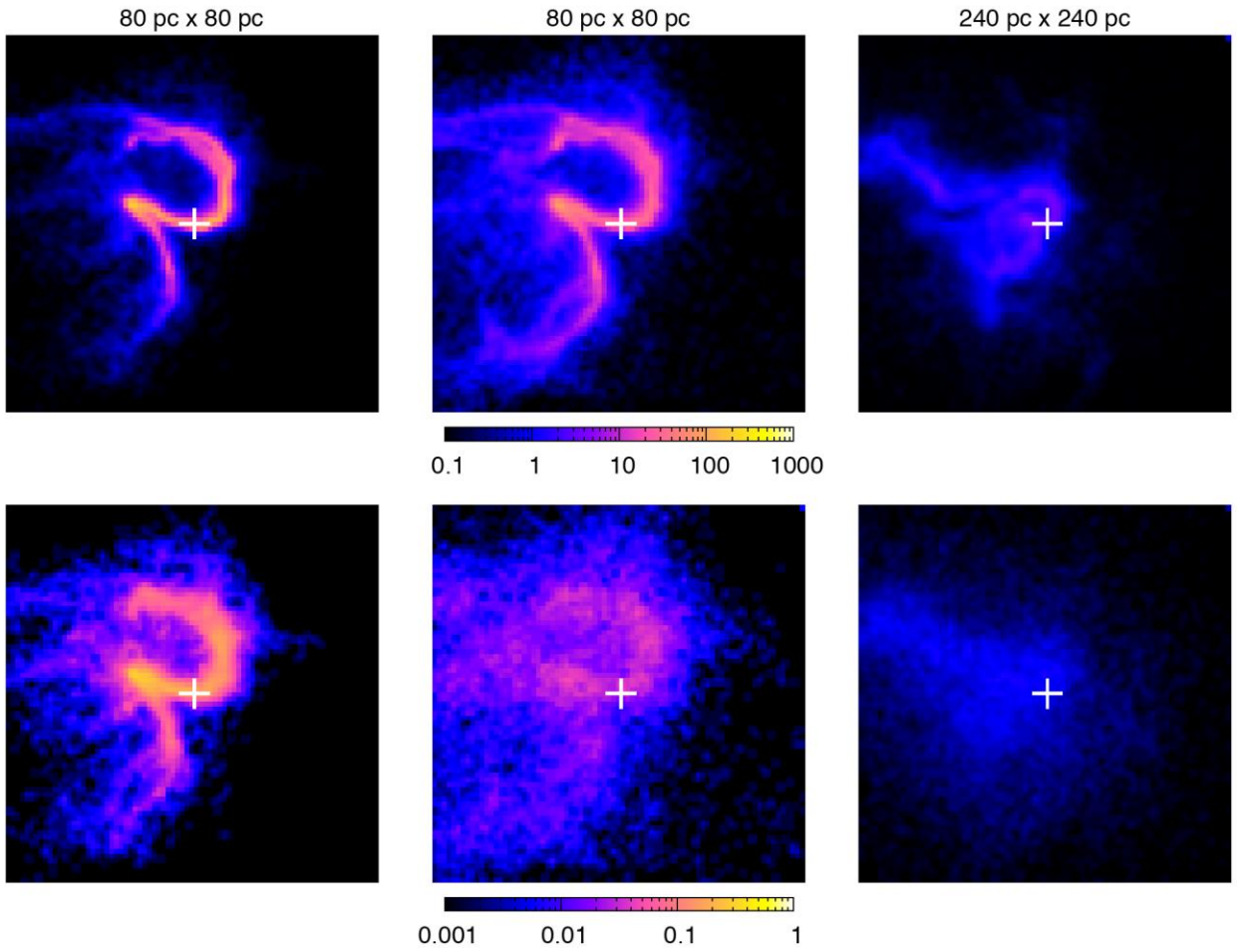

FIG. 5: Relative surface brightness in gamma-rays on the sky above $E_\gamma \geq 300\,\mathrm{GeV}$ (*upper row*) and $E_\gamma \geq 30\,\mathrm{TeV}$ (*lower row*) for a proton source, at $t = 0.5$, 2, 10 kyr after escape (*resp. left, middle and right columns*). For each row, see key below the middle panel. Same parameters and assumptions are used as for Fig. 4. White cross for the position of the source. The panel sizes are $80\,\mathrm{pc}\times 80\,\mathrm{pc}$ (*left and middle columns*) and $240\,\mathrm{pc}\times 240\,\mathrm{pc}$ (*right column*). Note the significant offset between the source position and the center of the extended gamma-ray emission on the two right panels.

arXiv:1306.3209v2 [astro-ph.HE] 26 Jul 2013

TeV cosmic-ray proton and helium spectra in the myriad model

G. Bernard et al., A&A **555** (2013) A48

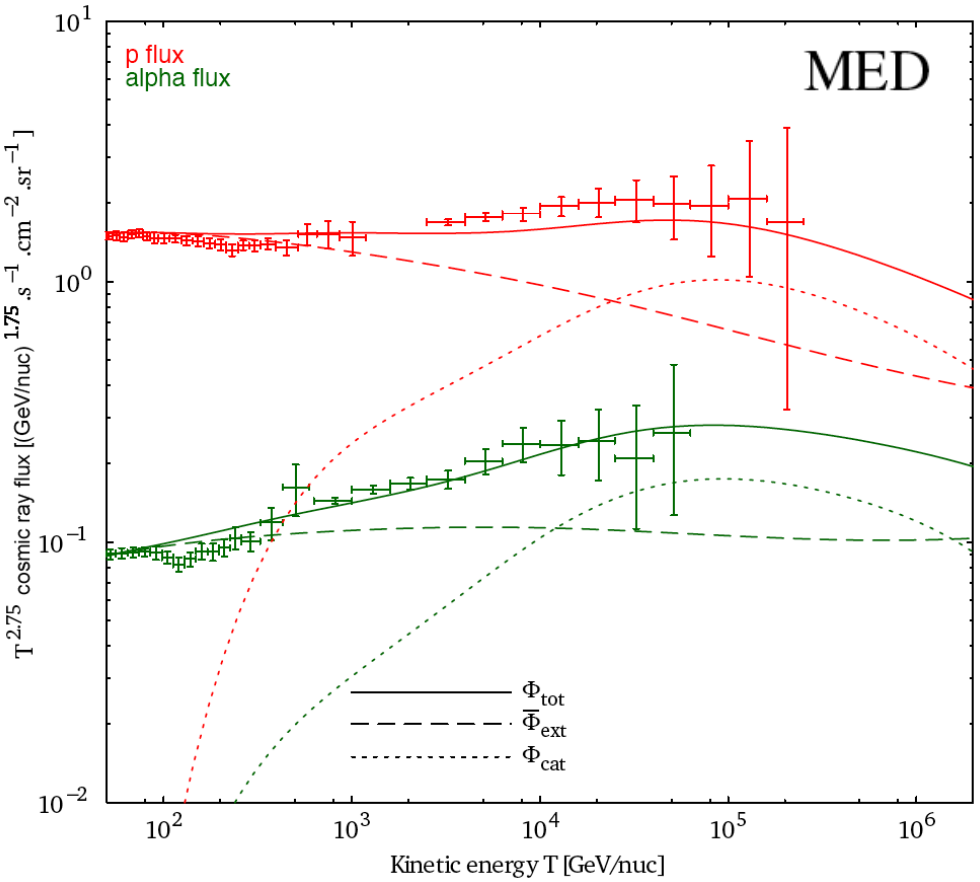

Model	K_0 [kpc^2/yr]	δ	L [kpc]	V_c [kpc/yr]	q_p^0 [GeV^{-1}]	q_{He}^0 [(GeV/n)$^{-1}$]
A	2.4×10^{-9}	0.85	1.5	1.38×10^{-8}	1.17×10^{52}	3.22×10^{51}
B	2.4×10^{-9}	0.85	1.5	1.38×10^{-8}	0.53×10^{52}	1.06×10^{51}
MED	1.12×10^{-9}	0.7	4	1.23×10^{-8}	15.8×10^{51}	3.14×10^{51}

model	$\alpha_p + \delta$	$\alpha_{He} + \delta$	ν [century^{-1}]	H injection	He injection	χ^2/d.o.f.
A	2.9	2.8	0.8	0.19	0.05	0.61
B	2.85	2.7	1.4	0.12	0.07	1.09
MED	2.85	2.7	0.8	0.148	0.07	1.3

Model	K_0 [kpc^2/yr]	δ	L [kpc]	V_c [kpc/yr]	q_p^0 [GeV^{-1}]	q_{He}^0 [(GeV/n)$^{-1}$]
A	2.4×10^{-9}	0.85	1.5	1.38×10^{-8}	1.17×10^{52}	3.22×10^{51}
B	2.4×10^{-9}	0.85	1.5	1.38×10^{-8}	0.53×10^{52}	1.06×10^{51}
MED	1.12×10^{-9}	0.7	4	1.23×10^{-8}	15.8×10^{51}	3.14×10^{51}
model	$\alpha_p + \delta$	$\alpha_{He} + \delta$	ν [century^{-1}]	H injection	He injection	χ^2/d.o.f.
A	2.9	2.8	0.8	0.19	0.05	0.61
B	2.85	2.7	1.4	0.12	0.07	1.09
MED	2.85	2.7	0.8	0.148	0.07	1.3

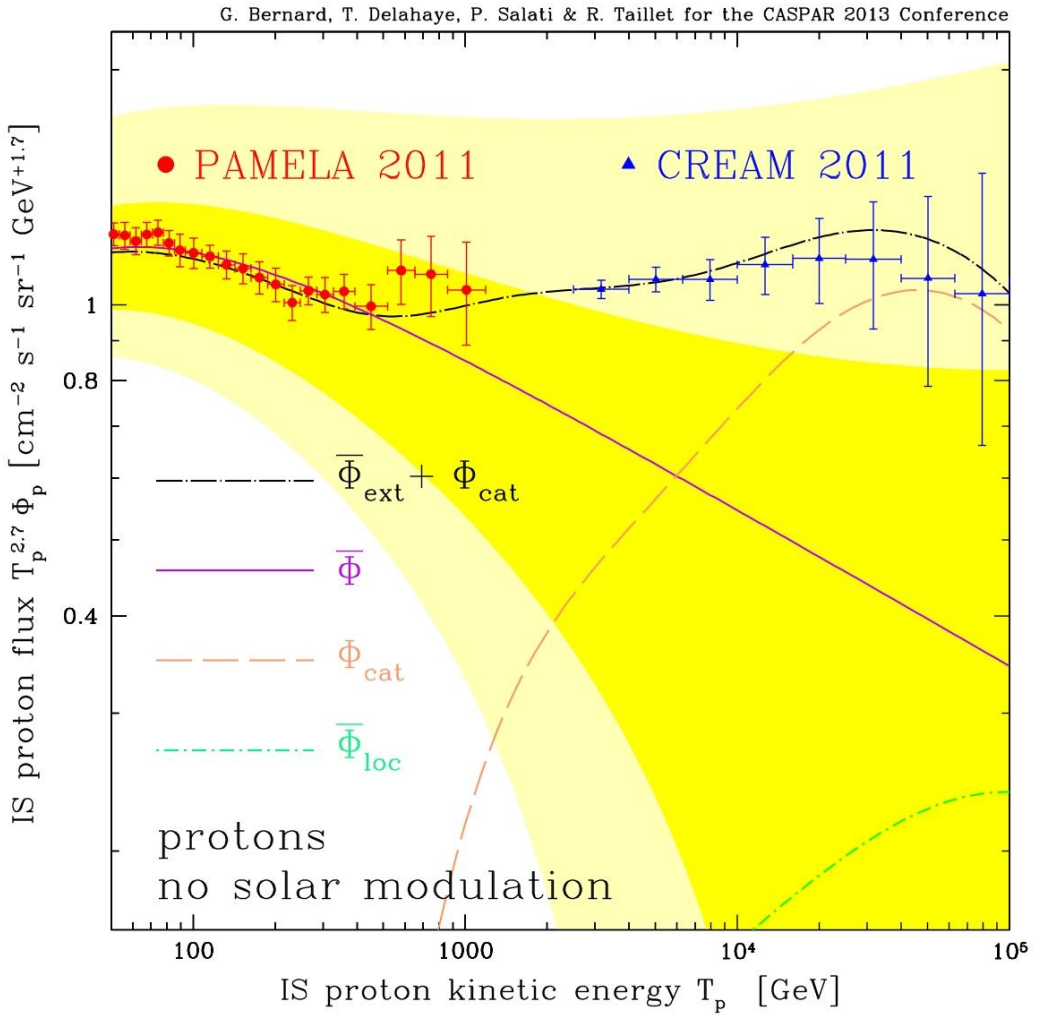

Model A - L = 1.5 kpc

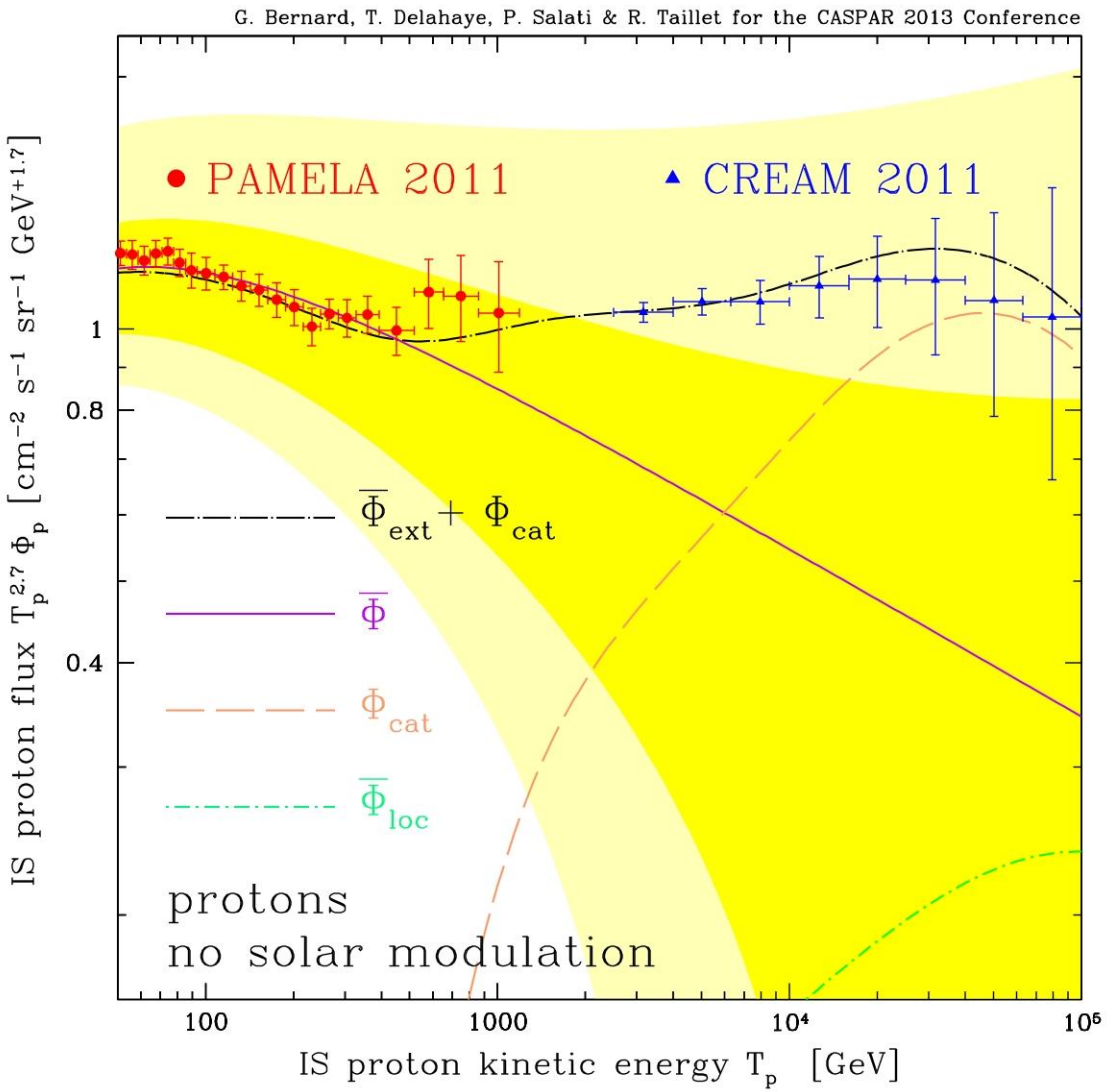

Model A - L = 3 kpc

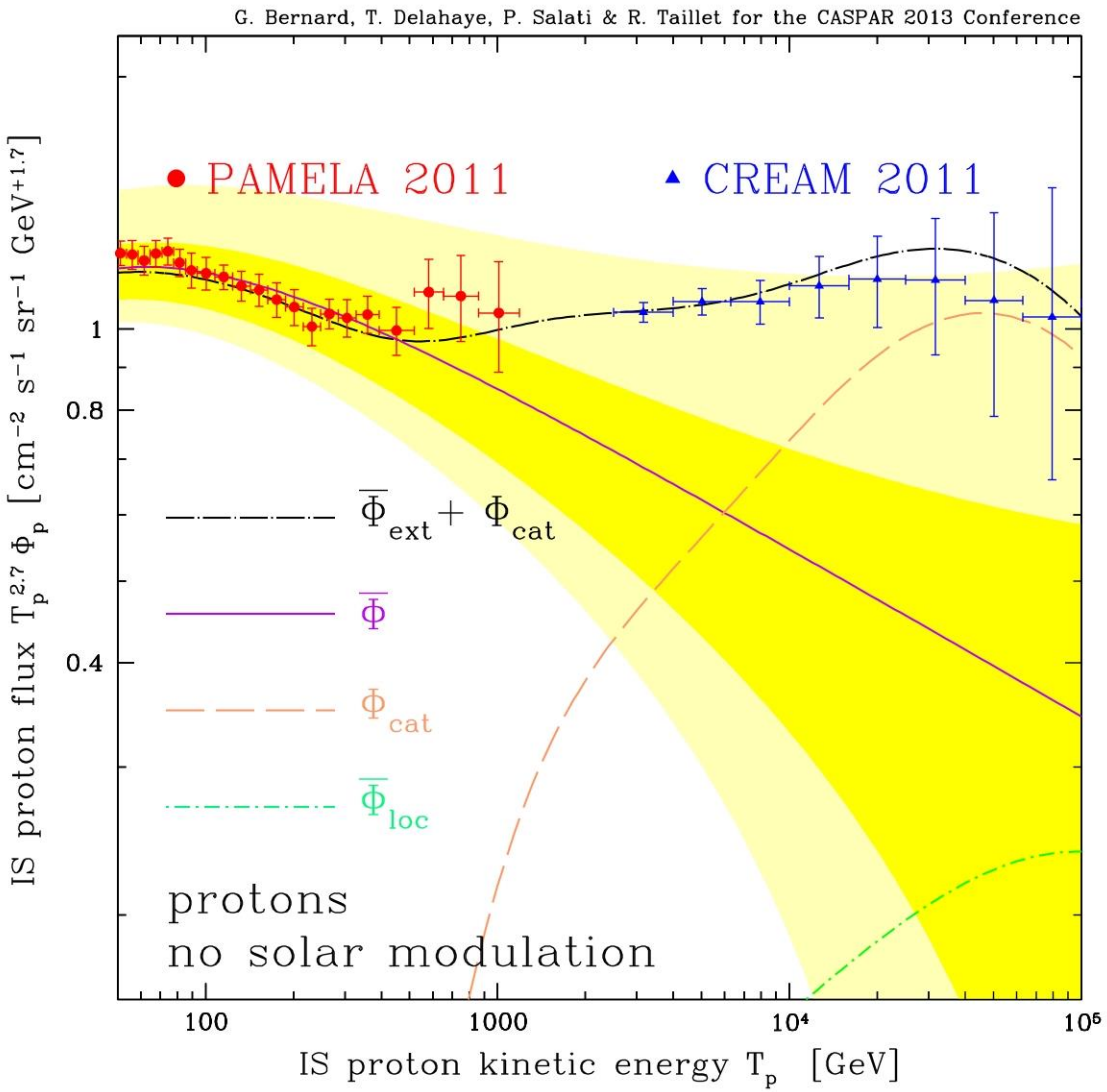

Model A - L = 6 kpc

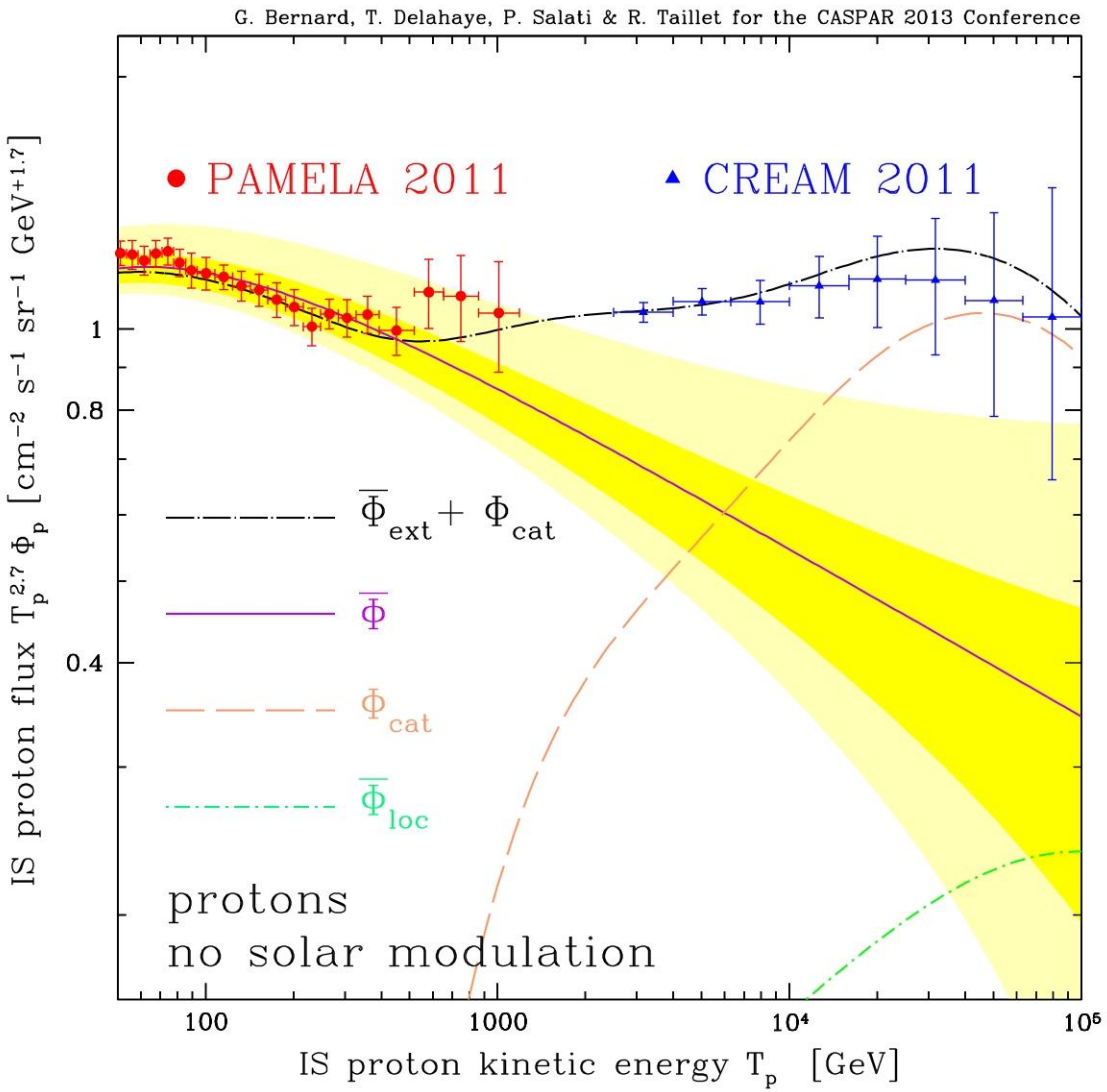

Model A - L = 9 kpc

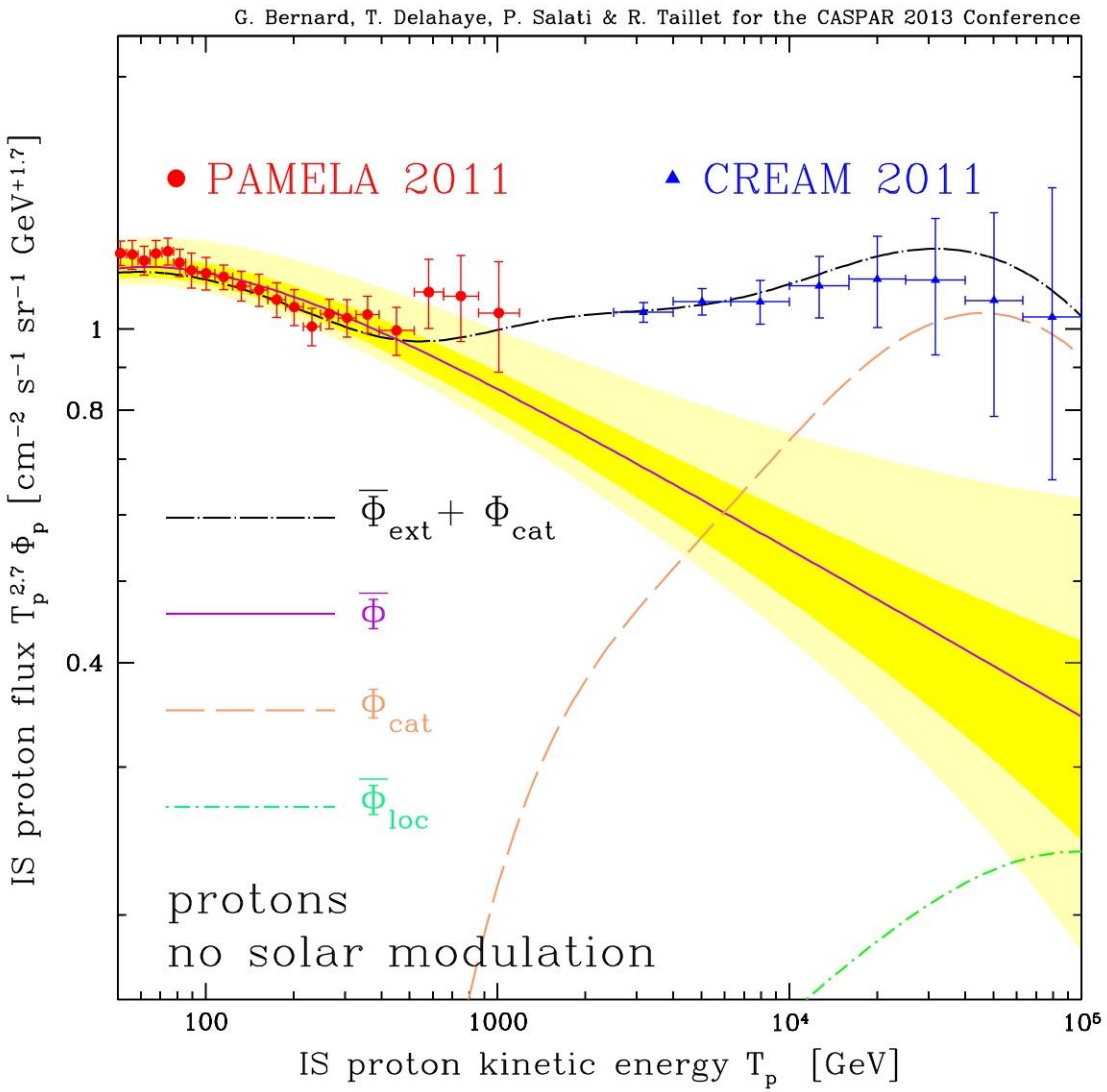

$$\tau_{\rm esc} = \frac{h}{V_C}\left\{1 - e^{-V_C L/K}\right\}$$

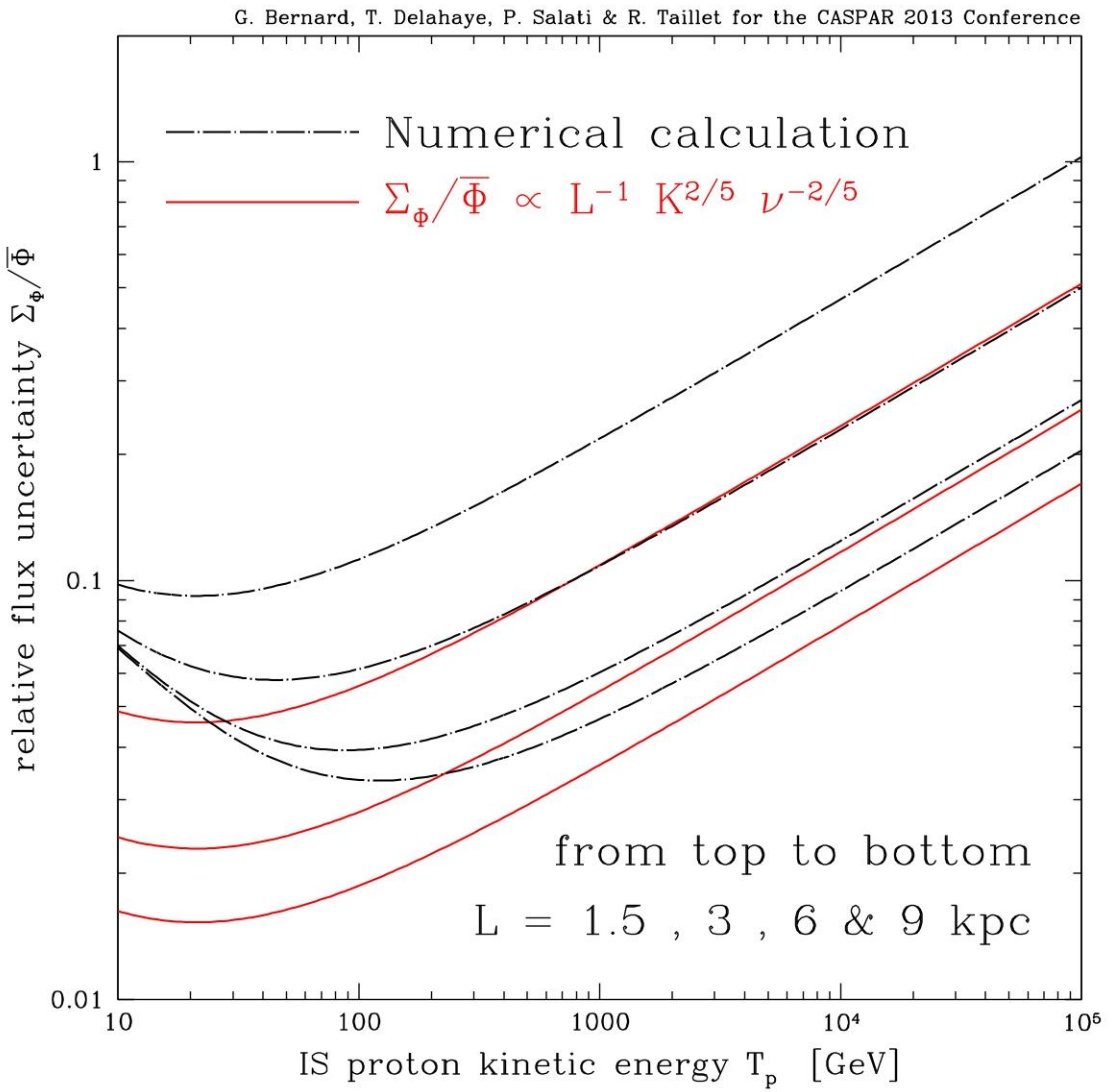

$V_C \times K^{-3/5} \times \nu^{-2/5}$

$L^{-1} \times K^{2/5} \times \nu^{-2/5}$

$$\tau_{\rm esc} = \frac{h}{V_C}\left\{1 - e^{-V_C L/K}\right\}$$

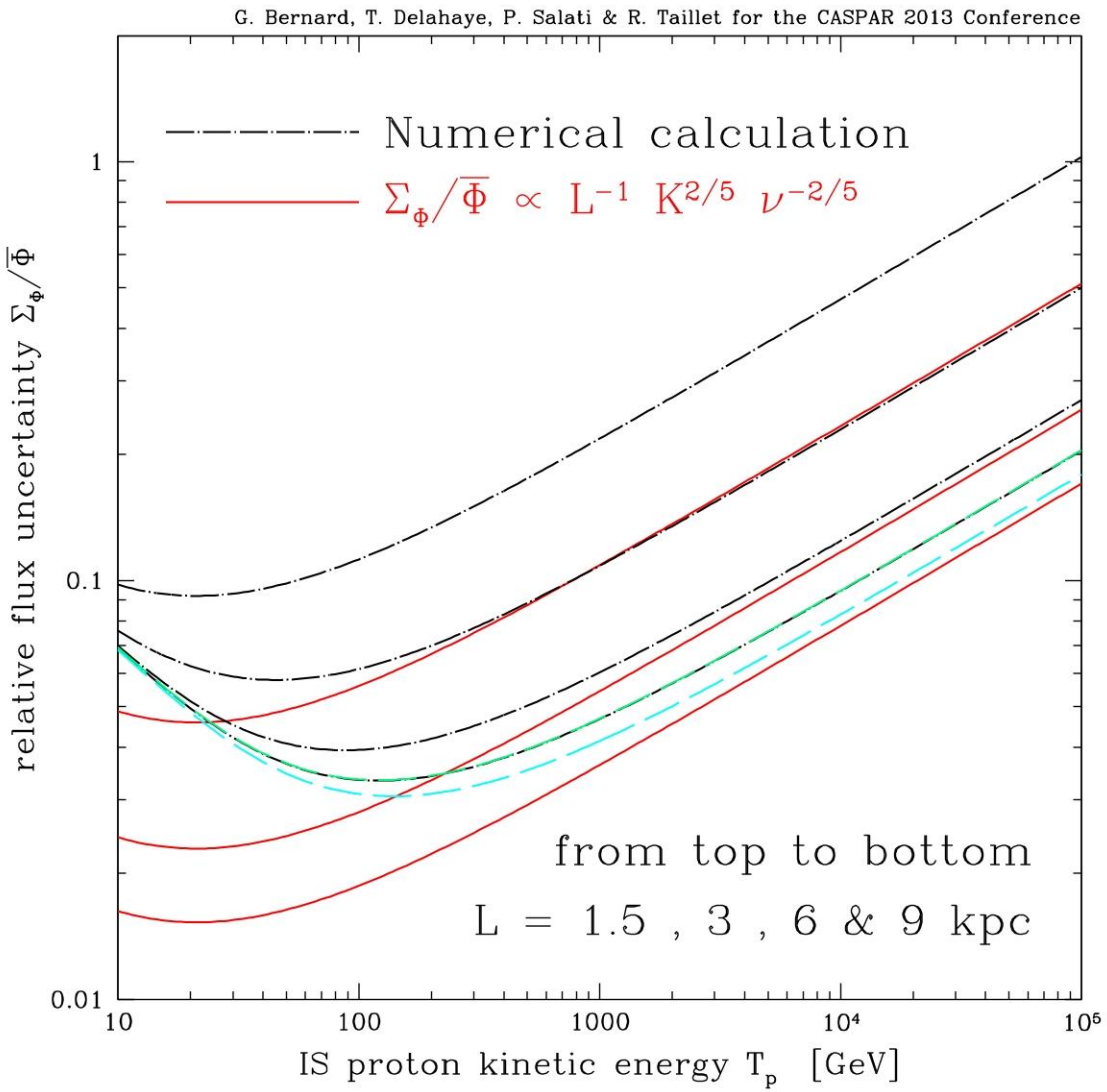

$V_C \times K^{-3/5} \times \nu^{-2/5}$

$L^{-1} \times K^{2/5} \times \nu^{-2/5}$